Fatigue Behaviour of Flax/Glass/Epoxy Hybrid Composites

By

Soroush Asgarinia

Structures and Composite Materials Laboratory

Department of Mechanical Engineering

McGill University, Montreal

June, 2014

A thesis submitted to McGill University in partial fulfillment of the requirements of the degree of Master of Engineering

Abstract

An experimental investigation of the fatigue behaviour of woven flax fibre hybridized with woven glass fibre, in an epoxy matrix, is presented. Three different hybrid compositions of flax fibre with glass fibre were manufactured using vacuum assisted resin transfer moulding. The hybrid composites are all five layer symmetric laminates $[0_w]_5$. All the laminates were tested under tension-tension fatigue loading conditions. The specific stress-number of cycles to failure (S-N curves) of all hybrid configurations were generated. The results were compared in terms of fatigue life, fatigue sensitivity, modulus decay and fracture mode of each hybrid laminate at different load levels. The results showed that introducing a small amount of glass fibre in a flax fibre laminate, improves the fatigue strength and fatigue life of the laminate. For the hybrids with partial replacement of glass fibre with flax fibre, the reduction in fatigue strength is evident compared to the plain glass fibre laminate. However, looking at the normalized S-N curve, good improvement on the fatigue life at low load levels and reduction in fatigue sensitivity is apparent. In summary, this work shows the potential for increased use of natural fiber materials in low-load bearing structures.

Résumé

Cette thèse présente une étude expérimentale du comportement en fatigue de composites hybride lin/E-glass/époxy. Trois différentes compositions hybrides fibres de lin/fibre de verre ont été fabriquées en utilisant un procédé d'infusion de type VARTM. Les composites sont tous symétriques à cinq couches $[0_w]_5$. Ils sont ensuite testés en fatigue avec un chargement de type tension-tension. Le nombre de cycles à rupture (S-N) de toutes les configurations hybrides ont été obtenues. Différentes propriétés des composites hybrides sont comparés pour plusieurs chargements, notamment la résistance en fatigue, la sensibilité à la fatigue, la diminution du module ainsi que le mode de rupture. Les résultats montrent que l'introduction d'une petite quantité de fibre de verre dans un laminé de fibres de lin améliore la résistance à la fatigue et le nombre de cycle maximum avant rupture. Pour les hybrides avec remplacement partiel des fibres de verre avec de la fibre de lin, la réduction de la résistance à la fatigue est évidente par rapport au stratifié uniquement à base de fibres de verre. Cependant, en regardant la courbe S-N normalisée, on remarque clairement une amélioration significative de la durée de vie en fatigue à faible charge et une réduction de la sensibilité à la fatigue.

Acknowledgments

I would first like to acknowledge my supervisor, **Professor Larry Lessard**, for giving me the opportunity to pursue this research. His support throughout this research was an invaluable asset, which made this research possible. I am also thankful for the help of **Dr. Steven Phillips**, who initiated the idea behind this research and his expertise was a vital factor in making this research a success.

I would like to extend my gratitude to **Ms. Azita Sirani** for her assist in proofreading this thesis, and my friend and colleague **Mr. Nils Cuinat-Guerraz** for helping me in translating the abstract.

Finally, I would like to thank my family who taught me the value of education and supported me with their continuous love throughout the years.

Table of Contents

List of figures

List of tables

List of equations

1. Introduction

The relatively new era of advanced materials has opened the field for many researchers to explore the diverse complexities of such materials. As for composite materials, their superior performance over traditional materials has given fibre-reinforced composites increased usage and has opened more avenues for research. Advanced composite materials, which are essentially high performance fibres embedded in one of many types of matrix materials, create countless possibilities for different combinations. Hybridization with more than one type of fibre within the same matrix gives fibre-reinforced composites another dimension of versatility. Cellulose/synthetic fibre-based reinforced hybrid composites is one of the many possibilities.

1.1. Natural fibres and their hybrids

Although natural fibres are among the oldest materials used by man, there is limited amount of investigation conducted to fully comprehend their behaviour. However, during recent years the need for developing more sustainable materials has created the incentive for researchers to study natural fibres [1]. Natural fibres are renewable, biodegradable and non-abrasive abundant sources as reinforcement materials, which have lighter weight and consume less energy during manufacturing and extraction compared to synthetic fibres [2]. Flax fibres are cellulose based bast fibres, which are among the most common natural fibres used in polymeric composites [3]. Ditterber and GangaRao [4], who have compared various natural fibres and overviewed their properties, have stated that among different natural fibres, flax fibres offer the best blend of lightweight, low cost and high strength and stiffness for structural applications. Due to their low density, they have promising specific mechanical properties, which are comparable to those of glass fibres [5]. Among flax producers, Canada is the largest producer and exporter of flax material [6], which makes it a great economical source. The current applications of natural fibres are in the automotive industry for sound abatement and paneling elements in airplanes and trains [7], [8]. Natural fibres exhibit excellent acoustic and thermal insulation properties, due to the presence of hollow lumen tubes in their fibre structure. Composite parts made out of natural fibres also exhibit better energy management characteristics compared to glass fibre reinforced composites [9]. In automotive parts, natural fibre composites not only reduce the mass of components, they also decrease the production energy consumption by 80% [10].

Nevertheless, moisture sensitivity resulting in fibre swelling, low impact resistivity and low thermal tolerance are drawbacks that cause limitations in the use of natural fibres. Another important disadvantage is the batch-to-batch variability of these types of fibre due to the uncontrollable forces of nature during the growing of the fibers. Factors such as plant growth conditions, maturity during harvest and fibre extraction technique, all affect the quality of the final product [11].

Many attempts have been made to remedy the drawbacks of natural fibres and increase their use, such as chemical [12], physical [13] and surface treatments [10]). One of the best ways to improve natural fibres according to Rouison [14] is by hybridizing natural fibres with small amounts of stronger synthetic fibres such as glass fibres. Hybrid composites have proven to create structures with a balanced effect from the reinforcing fibres. Hybridization can be considered as a viable solution to promote more extensive use of natural fibre reinforced composites in the near future.

1.2. Motivation

Natural fibre reinforced composites are being considered as an alternative to glass-reinforced composites because of their compatible mechanical properties while having lower environmental impact. Natural fibres offer environmental advantages such as reduction in use of non-renewable energy/material sources, lower emissions and greenhouse gas emissions, greater energy recovery and the biodegradability of components at disposal. To assess the environmental aspect of natural fibres, life cycle assessment (LCA) can be utilized, which studies the potential environmental impact of a material via tracing a product's life from 'cradle to grave'. A study done by Joshi et al. [15] shows the superiority of natural fibre reinforced composites compared to glass-reinforced composites in different application. Natural fibres consume 5 to 10 times less energy during their production compared to glass fibres. Furthermore, the increase in fuel efficiency caused by 20 to 30% weight savings gives natural fibres a great advantage over glass fibre components in transportation applications. Unlike glass fibres, natural fibres can be incinerated after their useful life. Incineration of natural fibres is considered to be CO_2 neutral, since the plant from which natural fibres are extracted consumes carbon di-oxide during its growth. However, these environmental advantages become feasible only if the components made

out of natural fibre composites endure a minimum useful lifetime. As Corbiere-Nicollier [2] reports, the use of China reed fibre reinforced in plastic proves to be advantageous from an ecological point of view only if the pallet made out of China reed fibre composites has a minimum lifetime of 3 years. This is a great indication of the vital need to study the durability of natural fibres and better fit them in applications that suit them best.

Nunna et al. [16] summarizes the research done on natural fibre hybrids and the factors affecting their mechanical behaviour. All studies report improvements by hybridization of natural fibres with synthetic fibres in terms of better flexural and axial strength, better impact resistance and less degradation due to environmental effects. These higher performance materials also take advantage of the good properties of the natural fibres, such as sound isolation capabilities and higher damping properties. As a result, with a proper design a hybrid composite with a balance between performance and cost can be achieved, where the advantages of one type of fibre complements what is lacking in the other.

Despite numerous promising achievements at the laboratory scale, some challenges are still preventing bio-composites from entering industrial scale production and use. One major obstacle preventing the successful commercialization of natural fibre reinforced composites is the lack of information and data on the durability of these materials. Durability is defined as the resistance to deterioration against external causes as well as internal causes. Here, external sources refer to the effect of environment on the composite, and internal causes refer to damage developed inside the composite part as it experiences different types of loading. Natural fibre hybrids, suffer most from this lack of data due to the complexity of such studies and the variety of fiber possibilities. Durability against internal causes, or in other words the fatigue resistance of a material, has become more critical as designs have evolved to more efficient designs that push the materials to their limit [17]. Hence, the need for these types of studies is apparent.

1.3. Objective

Objectives of this research were selected to assess the effect of hybridization of natural fibres, such as flax, with synthetic fibres, such as glass, and to find the best combination with the best fatigue performance. Although this research might appear to be a case study rather than a general case, the effort has been put to generate practical and repeatable data in order to make the

generated data implementable for other cases. Utilizing woven fabrics, rather than random strand mats which have been mostly used in previous studies, and using strong matrix systems such as epoxy are all attempts to make this study closer to real world applications. This report aims to promote the potential use of natural fibres for more advance structures, such as aircraft interior structures, which require a lightweight material with sound abatement properties, while maintaining an acceptable durability and strength. The objectives are set as follows:

- Study the effect of partial replacement of flax fibres with glass fibres in terms of fatigue performance.
- Create a glass dominant hybrid laminate to study the effect of introducing flax fibres in a glass fibre laminate.
- Assess the damage accumulation mechanism during fatigue cycling in different laminates.
- Study the fracture behaviour of different hybrids.

1.4. Thesis organization

This thesis consists of the following chapters: First, chapter 2 provides some background information about natural fibres and their hybrids, and then a review of the relative studies done on the fatigue behaviour of natural/synthetic hybrid composites is presented. In the subsequent chapter, chapter 3, the experimental method is presented which provides details on the manufacturing steps taken for making the hybrid laminates. In the same chapter, information on the quality of the manufactured samples and the testing procedure is provided. Then, chapter 3 and 4 present the results and the discussion, which discusses the fatigue behaviour and the effect of hybridization on damage mechanism according to the gathered results. Finally, chapter 5 provides a conclusion summarizing what has been done, contributions made and potential future work.

2. Literature Review

The natural fibre category encompasses a wide range of fibres, sourced from plants, animals and minerals. Plant based or lignocellulosic fibres, which are the most frequently used type of natural fibres as reinforcement in polymeric matrices, can be extracted from the stem, leaf or the seeds of plants [18]. Flax fibres, extracted from the stem of flax plants, exhibit the best combination of low cost, low weight and high strength when compared to other plant fibres [4]. Properties of lignocellulosic fibres mainly depend on the type of the plant, the growth site, age of the plant and the extraction method used. The main constituents of a lignocellulosic fibre are cellulose, hemi-cellulose and lignin in varying quantities. Cellulose is the hydrophilic part of the plant, which provides strength and stiffness to the plant cell wall [11]. Hem-cellulose is an amorphous polymeric part of the plant, and lignin is the bonding agent holing fibre bundles together. By combining such fibres with stronger manmade fibres within a laminate, a hybrid composite can be achieved that takes advantage of the best of both fibre types. Nevertheless, these advantages are not absolute and are bounded by the properties of constituent fibres exhibited in a single-fibre laminate. Therefore, a proper design is required to achieve a balance between the properties.

Depending upon the arrangement of the fibres inside a hybrid composite, different types of hybrids can be achieved. Intermingled, interlaminated and interwoven are some examples of methods that are used to produce a hybrid type material. In this research, interlaminated hybridization has been used, which is defined as a hybrid laminate where different layers, each consisting of one type of fibre only, are stacked together and are imbedded inside a matrix. Chou discusses the important effects of hybrid composites in his book, the Microstructural Design of Fibre Composites [19]. Effects such as stress concentration due to the sequential failure of different types of fibres in a hybrid laminate and load redistribution, tensile stress-strain behaviour and strength prediction theories. Concerning strength theories, considering that the fibres used in a hybrid composite have different mechanical properties, the behaviour of the resulting composite can simply be predicted by the rule-of-mixtures. Defining one fibre as being low elongation (LE) and the other as high elongation (HE), the rule-of-mixtures can be defined as below when the failure of LE fibres results in total failure of the laminate:

$$\sigma_{cu} = \sigma_{Lu} V_{LE} + \epsilon_{Lu} E_{HE} V_{HE} \qquad \text{Equation 2-1}$$

Where σ is the ultimate tensile strength, V indicates the fibre volume fraction, ϵ is the strain and E is the Young's modulus. The subscripts c denotes the values belonging to the whole composite, and L and H denote the low elongation and high elongation components. Another form of the rule-of mixtures, which is basically a weighted average of constituent properties, can be used to calculate the resultant elastic modulus of the hybrid laminate (Equation 2-2). The deviation from the rule-of-mixtures is considered as a hybrid effect.

$$E_c = E_{LE}V_{LE} + E_{HE}V_{HE} \qquad \text{Equation 2-2}$$

Other than just a deviation from rule-of-mixtures, others have defined the hybrid effect as a phenomena where a hybrid laminate can have a higher failure strain value than the LE fibres [20]. This possibility occurs when after the failure of LE fibres, HE fibres can still withstand the amount of applied load. In the case of an adequate adhesion between fibres and matrix, the stress gets redistributed back to the failed LE fibres, which also causes this pseudo ductile effect [19].

Considering both definitions for the hybrid effect, Marom et al. [21] investigated possible parameters that might be affecting the hybrid laminate other than the most commonly studied parameters such as relative fibre volume fraction of constituents. To isolate the effect of mechanical properties by minimizing the interface effects, a hybrid laminate with 50/50 wt.% of two types of carbon fibre with similar surface characteristics was tested. Results showed no hybrid effect in such a hybrid suggesting that similar interfaces would result in a hybrid laminate such that its static properties are predictable by averaging the components' properties. To investigate the effect of interface and number of layers, hybrid laminates with 1/1, 2/2, and 5/5 layer compositions of glass fibre and carbon fibre were tested. While no hybrid effect was observed in the elastic modulus, a positive hybrid effect for strain-to-failure and a negative hybrid effect for ultimate strength was reported. The positive hybrid effect for the strain was in terms of an increase in the maximum strain at failure of the hybrid laminate compared to the lowest strain-to-failure fibre component. As for the ultimate strength, the negative hybrid effect was in term of negative deviation from the rule-of-mixtures. As for the effect of layering, better results were observed in hybrids with more distinct and segregated stacking sequences.

Having provided some fundamental knowledge about hybrid composites, the following section will present a few studies done on natural/synthetic hybrids. While numerous studies on static

properties, such as tensile strength and impact resistance, of different natural/synthetic hybrids can be found, there are only few studies that investigate the fatigue behaviour of such hybrids. In the last section of this chapter, studies on the fatigue behaviour of natural/synthetic hybrids are presented in addition to one comparative study, which discusses the differences between fatigue behaviour of glass fibres and flax fibres.

2.1. Natural/Synthetic hybrids

Starting from some of the early studies done on natural/synthetic hybrids, Thwe and Liao [22] revealed noticeable enhancements of mechanical properties and durability of short bamboo fibres by mixing them with small amounts of glass fibre. In this study, short bamboo fibres were hybridized with 20% (by mass) glass fibres, reinforcing polypropylene (PP) and manufactured using compression moulding. The effect of utilizing anhydride polypropylene (MAPP) as a compatibilizer is also presented in this study. The results show an increase in flexural and tensile modulus up to 12.5%, and improvement in flexural and tensile strength by 25% after incorporating glass fibres with bamboo fibres. The effect of the MAPP compatibilizer is more evident in flexural properties compared to tensile properties, since changes in interlaminar properties play a more important role on the former properties. In terms of sorption behaviour and environmental aging effects on tensile properties, a 4% drop in saturated moisture level of Bamboo-glass fibre hybrid was observed. Moreover, smaller reduction in tensile strength and modulus was observed for the hybrid composite compared to plain bamboo PP composite after being aged in water for 1200 hours. Hence, hybridization can be also considered to improve the durability of natural fibres against environmental effects. In another study, Thwe and Liao have compared the fatigue behaviour of plain bamboo fibre laminate with the bamboo-glass fibre hybrid laminate, which is presented in the next section.

There have been many reports on improvements of natural fibre's mechanical properties as well as enhancements in impact resistivity after hybridization. Sreekala et al. [23] investigated the hybridization between randomly oriented oil palm fibre with glass fibre in phenol formaldehyde resin on its mechanical properties and the effect of the fibre volume fraction. Layers of the hybrid laminates were arranged in such a manner as to get the maximum intermingling between the fibres. Using hand lay-up technique followed by compression moulding allowed achievement

of different volume fractions. The best properties among all hybrid compositions were achieved when the fibres were mixed at 0.26:0.74 volumetric ratio of glass fibre with oil palm fibre with total fibre loading of 40 wt. %. The experimental results were compared with theoretical predictions using the rule-of-mixtures. A negative hybrid effect was seen in tensile strength and modulus while elongation at break shows a positive hybrid effect, which agrees with the findings of Marom et al. [21].

In the most recent study conducted by Atigah et al. [24], hybrid composites of kenaf-glass (KG) fibres reinforced in unsaturated polyester manufactured using a sheet moulding compound process were tested for tensile, flexural and Izod impact strength. The effect of fibre treatment with sodium hydroxide was also investigated. In this study, in addition to neat kenaf fibre and glass fibre composites, hybrids with different volumetric ratio of each component were manufactured. Results showed that the hybrid composed with 15 % treated kenaf fibres and 15 % glass fibre in a laminate with 30 % fibre volume fraction has the highest properties with the best interfacial bonding between the matrix and reinforcement among all other compositions. Fractography done on the failed specimens scanning electron microscopy showed fibre cracking, debonding and fibre pulled-out as the major fracture mode of laminates.

Another important aspect in this research involves what has been studied by Aabdul Khalil et al. [25], which is the effect of layering arrangement in a hybrid composite. In this study, the mechanical properties of oil palm of empty fruit bunch fibres (EFB) laminated at different layer arrangements with glass fibre (CSM) composites in the vinyl ester matrix system were investigated. The EFB and CSM fibres, hybridized by equal weight fractions, were laminated using six different layer arrangements, and were manufactured by resin transfer moulding (RTM). Unfortunately the author neither reports any fibre volume fraction of the manufactured laminate, nor does the study show any clear indication of how equal weight fraction was achieved. Thus, a firm statement cannot be made related to the quality of the parts. The mechanical and physical properties in terms of tensile, flexural, impact resistance, water absorption and dimensional stability were investigated in this study. Hybrid composites with glass fibres at the outer layer exhibited higher tensile and flexural properties, while higher impact properties was seen in composites with natural fibres at the outer layers, which contradicts results done by other researchers on the impact resistance of natural/synthetic hybrid composites.

As for physical properties, the laminates with glass fibres at the outer layers also showed lower water absorption and better dimensional stability.

Sabeel Ahmed and Vijayarangan [26] have conducted more accurate research on the effect of stacking sequence. Six different stacking sequences were studied in terms of tensile, flexural and interlaminar shear properties. Hybrid laminates consist of a total of 10 plies were made out of woven glass and jute fabrics reinforcing polyester resin using hand lay-up technique. The results indicate that the properties of jute composites could be significantly improved by integration of glass fibre as extreme plies. While the layering sequence has minimal effects on the tensile properties, flexural and interlaminar properties showed greater sensitivity. Finally, the author suggests that a hybrid laminate with two extreme glass plies on both sides could be the most optimum mixture with a good balance between the properties and cost. Therefore, according to the two above-mentioned studies, there exist good incentives to place synthetic fibres at the outer layers while hybridizing with natural fibres.

Looking for a balance between cost and performance, Cicala et al. [27] presents one of the few research works done on real work applications of natural/synthetic hybrid composites. Composite laminates made out of epoxy vinyl ester resin reinforced with combination of woven glass fibre and matted hemp fibres were tested for pipeline fittings applications in chemical plants. Despite the low fibre fraction (8-11%) achieved by the hand lay-up manufacturing technique used, the designed hybrid fitting exhibited promising results under real work conditions by withstanding an internal pressure of 10 bar in the presence of acid aqueous solutions. The adoption of this design allowed for a 20% cost reduction and 23% weight saving compared to the available commercial solution. This is a valuable research effort that shows the potential of hybrid composites utilizing natural fibres.

2.2. Fatigue in hybrids

It is believed that high strength brittle fibre construction of composite materials should not experience fatigue; however, throughout the years, research and experience have shown otherwise. These studies have shown that regardless of the type of the fibres, as cyclic loading takes place small viscoelastic movements inside the resin can result in local redistribution of stress and hence allow some random fibre damage [28]. Nevertheless, inhomogeneous composite

materials have different fatigue mechanisms compared to metals. Unlike metals, where fatigue failure occurs by the propagation of a single micro-crack, composite materials accumulate damage in a rather general manner by developing many random cracks. Cracks causing delamination, fibre failure, transverse-ply cracking and many other types of damage accumulations can lead to final fatigue failure. In this section, research done on the fatigue properties of hybrid composites containing natural fibres are presented.

Thwe and Liao extended their study on the bamboo-glass fibre reinforced polypropylene hybrid composite (BGRP) by studying their hygrothermal aging and their fatigue behaviour under cyclic tensile loading [29]. Injection moulded samples were studied for their tensile behaviour before and after aging, their sorption behaviour and fibre and matrix degradation by hydrothermal aging. Also, Fatigue fracture surfaces of selected samples were inspected under scanning electron microscope (SEM) for damage and failure characterization. Considering the fatigue life of bamboo fibre reinforced polypropylene (BFRP) with 20 wt.% fibre content, and BGRP laminate with 15 wt.% bamboo fibre content and 5 wt.% glass fibre content, minimal improvement was observed by introducing glass fibres to the bamboo fibre laminate. In regards to the damage development during cyclic loading, tensile stiffness degradation was measured. It was shown that hybridization have improved the damage resistance by lowering the slope of the stiffness degradation curve.

On the investigation of flexural behaviour of natural/synthetic hybrids Reis et al. [30] reported on the fatigue behaviour of such hybrids in addition to the study of flexural properties. Hybrid laminated composites consist of non-woven hemp fibre/polypropylene at the core and two layers of woven glass fibre/polypropylene at the surface layers were compared against a non-hybrid laminate manufactured from the same glass fibre/polypropylene fabrics used in the hybrid laminate. Despite lower flexural strength and elastic modulus of the hybrid laminate composite by 4% compared to the non-hybrid laminate composite, due to the lower specific weight of the hybrid composite, it has almost 22% higher specific static stiffness and strength. Also, looking at the fatigue strength, although the advantage is minor in this case, the hybrid laminate has higher specific fatigue strength. This paper also studies the variation in stiffness modulus during fatigue loading. The non-hybrid laminate exhibits a significant drop at the early stages followed by a slow decrease until failure. As for the hybrid laminate, while the sudden drop at the initial stage

does not exist, the overall decay in the modulus has the same intensity. From the results of this study, the authors conclude that by taking the economical and ecological benefits of these types of hybrid laminates into consideration in addition to their high specific properties, they can be considered as promising materials for structural applications where bending loads dominate.

Shahzad [31] tested the impact and fatigue properties of hemp-glass hybrids in unsaturated polyester matrix made by hand layup followed by compression moulding. He tested two different laminate compositions, one sandwiching the hemp fibre between two layers of glass and other being hemp fibres on the skin and a layer of glass fibre in between. Replacement of about 11% of hemp fibres with glass fibres in the hybrid composite increased the impact damage tolerance by more than double at 4 j impact. As for fatigue performance, the hybrid composites showed improvement in fatigue strength without any improvement in fatigue sensitivity. The fatigue sensitivity coefficient is defined as the slope of the normalized S-N curve. While the glass-skin hemp-core composite shows better improvement in fatigue strength and impact resistance, it has a steeper S-N cure and hence considered to be more fatigue sensitive. Thus, the author suggests that placing hemp fibres at the skin and glass fibres at the core could be a more efficient method of improving the fatigue strength of hybrid composites.

Since there are very few studies done on the fatigue behaviour of natural/synthetic hybrids, it is worth looking at some comparative studies done on the differences between natural and synthetic fibres. Yuanjian and Isaac [32] studied the fatigue and impact performance of laminates made out of hemp fibre mats reinforced with polyester, and they compared the results with glass fibre reinforced polyester composite samples. Although this is not a study on hybrid composites, in addition to just looking at the fatigue and impact properties, tensile modulus degradation during fatigue cycling was also presented, which is a good indication of the damage accumulation. For all glass fibre composites, a steady decrease in modulus was observed as the number of fatigue cycles increased. In contrast, hemp fibre composites showed a relatively steady modulus throughout fatigue cycling, which shows stability of hemp fibres as compared to glass fibres.

Liang et al. [33] compared the fatigue life of flax and glass fibres in an epoxy matrix (FFRE and GFRE consequently). Samples made by compression moulding, having $[0/90]_{3S}$ and $[\pm 45]_{3S}$ stacking sequences, were tested under tension–tension fatigue loading. He concluded that within the studied life range, the $[0/90]_{3S}$ specimens of flax fibre laminates had lower fatigue endurance

than glass fibre laminates, but the $[\pm 45]_{3S}$ flax fibre reinforced polymers showed better specific fatigue endurance than glass fibre laminates. FFRE also showed superior fatigue performance when looking at the normalized fatigue life by the tensile strength, for both stacking sequences. Moreover, flax fibre showed more stable cyclic performance than glass fibres by exhibiting less permanent deformation. The study also presents the stiffness degradation during cyclic loading. Unlike glass fibres with a three-stage stiffness degradation, FFRE specimens showed a stiffening phenomenon, which could be related to the straightening of the microfibrils.

In a more recent study by Fotouh, A.A et al. [34], the fatigue behaviour of chopped hemp-fibre-reinforced High Density Polyethylene (HDPE) composites in different volume fractions (13.5% and 30.1%) was investigated. Fatigue tests have been conducted at two stress ratios (0.1 and 0.8) and many stress levels, which provide the reader with good set of data points. While the type of material and the matrix investigated in this study is different than what Liang studied, the fatigue behaviour of natural fibre reinforced composites in both cases seems to be matrix dominant with similar failure mechanisms.

Based on the literature review, one can see that there is a lack of clear knowledge on the fatigue behaviour of natural/synthetic hybrids despite the promising results on the improvements achieved by such hybridizations in terms of static properties and environmental stability. Therefore, there is a great incentive to fill the existing gap by studying the fatigue behaviour of mentioned hybrids.

3. Experimental Method

This chapter will present a detailed overview of the approach taken in this research to achieve the mentioned objectives. First, hybrid composites studied in this research will be presented followed by the reasoning for each composition. Then, a descriptive step-by-step manufacturing procedure is presented consisting of raw material preparation, manufacturing technique and sample preparation. Finally, the tensile and fatigue testing methods are discussed.

3.1. Hybrid compositions and approach

To study the effect of hybridization between natural and synthetic fibres on their fatigue performance, three different hybrid compositions were proposed. All laminates are five layers of 0-degree woven fabric where different hybrids were created by stacking different ratios of each material in a laminate. The angle was calculated based on the warp orientation. In addition to hybrid compositions, non- hybrid laminates of flax fibre reinforced epoxy (FFRE) and glass fibre reinforced epoxy (GFRE) were considered as baselines. Figure 3.1 shows the different configurations where [F] corresponds to a single layer of flax fibre and [G] stands for a single layer of glass fibre. For instance, [G/F_3/G] represents a laminate with three layers of flax fibre fabrics that are covered by single layer of glass fibre on each side. The same notation is used throughout this report to refer to different laminates.

Three different hybrids can be seen in Figure 3.1. The [F_2/G/F_2] hybrid laminate is a flax fibre dominant hybrid composite, where the aim is to study the effect of partial replacement of flax fibres with glass fibres. On the same note, the glass fibre dominant hybrid composite [G_2/F/G_2] was designed to study the effect of partial replacement of glass fibres with flax fibres. Replacing the middle layer in both compositions creates a symmetric hybrid laminate.

Previous studies done on natural/synthetic hybrid composites tend to agree on gaining more from the hybridization when stronger synthetic fibres are placed at the outer layers. Better impact resistance [35], increase in the tensile and flexural strength [26] and lower water absorption [25] are all positive effects of placing glass fibres at the most extreme layers. Knowing the advantages of these existing hybrids, the [G/F_3/G] hybrid laminate was proposed in order to study its fatigue behaviour.

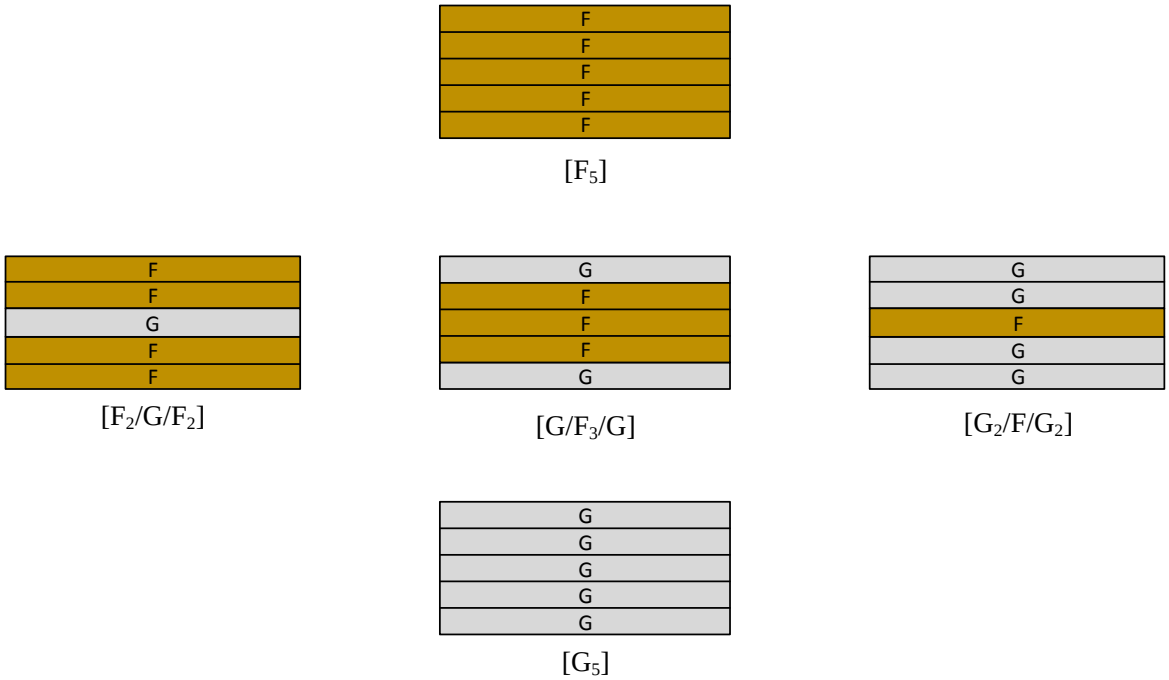

Figure 3.1 All considered laminates, with their layer composition. "G" stands for a glass fabric layer and "F" stands for a flax fabric layer

3.2. Material specifications

Both flax fibres and glass fibres were provided in woven fabric form. Flax material was kindly provided by JB Martin Ltd in Canada. It was a 2-by-2 twill weave fabric, 230 tex in warp and weft direction with an areal weight of 224 g/m^2. The crimp index and twist of the fabric were measured by image analysis. The values are consequently 1.6% (0.64) and 42.15 (3.66) twist per meter, equal in warp and weft direction. For details on crimp and twist measurements, refer to Appendix I. The plain weave E-glass was provided by Bell helicopter Canada. The glass fibre mat had an areal weight of 205 g/m^2. The matrix was an 820 epoxy resin laminating system with 834 hardener, from CASS polymers. The resin data sheet can be found in Appendix VIII.

3.3. Manufacturing technique

Vacuum assisted resin transfer moulding (VARTM) is part of the liquid composite moulding category, in which liquid resin is drawn through the dry reinforcement by creating vacuum inside

the mould. Its advantage over more traditional manufacturing processes, such as hand layup, has made it more suitable for creating more complex parts in a cleaner fashion. First of all, less resin is required compared to the hand layup process and secondly, there is no direct contact with harmful resin and its emissions [36]. Higher volume fraction is achievable by VARTM compare to vacuum bagging, and it is more economical than traditional RTM processes since less tooling is required. Nevertheless, dimensional instability, low repeatability and lower material performance compared to autoclave manufacturing have limited its use [37]. Compaction pressure applied on the preform is via the pressure difference between the atmospheric pressure and the vacuum pressure inside the mould. Thus, using a flexible vacuum bag on one side is inevitable. Low rigidity of the vacuum bag causes thickness variation due to the in-plane pressure difference between the vent and the inlet port [36]. Many attempts have been performed to reduce this thickness disparity including controlled atmospheric pressure resin infusion (CAPRI). Higher volume fraction, by introducing a debulking step prior to the infusion, and reduction in thickness gradient by removing pressure from the resin reservoir and consequently decreasing the in-plane pressure difference are the improvements over the VARTM process [38]. Seeman composites resin infusion moulding process (SCRIMP) is another variation of VARTM process in which the resin flow is assisted by introducing a high permeable surface layer to the laminate [37]. Vacuum infusion technique used in this thesis is a combination of different techniques. These will become more clear from the detailed explanations of the steps that follow.

3.4. Raw material preparation

In this section, steps taken prior to the infusion will be discussed in detail. Fabric cutting and drying are the steps taken before preparing the setup to draw the resin into the dry reinforcement.

3.4.1. Fabric cutting

Fabrics were cut into 28 x 28 cm preforms using an electric scissor. Good care was taken to cut the preforms exactly perpendicular to the weft and warp of the fabric to eliminate the angle deviation from 0 degrees. This was achieved by carefully laying the fabric on a flat table to eliminate any pre deformation, and by removing one weft strand at a desired dimension to indicate the cutting path. The same technique was done in the warp direction. Using electric

scissors not only made the cutting process faster, but it prevented any in-plane shearing and deformation of the fabric.

3.4.2. Drying

Drying the fibres is an important step when dealing with natural fibres, since hydrophilic Cellulosic fibres have tendency to absorb significant amounts of moisture. The moisture content of the fibres varies between 5 to 10% [3]. This can lead to dimensional disparities in composites and also affects the mechanical properties. Also, this moisture could cause bad fibre-to-resin adhesion, due to the hydrophobic nature of matrix systems, and can create voids during the curing stage by evaporation [39]. It is also an unneeded source of weight, which is easily removable.

As stated earlier, CAPRI can create laminates with better volume fraction by performing debulking cycles on the preform before infusion. Debulking reduces the spring back effect of the fibres' stack, resulting in a thinner laminate with higher fibre volume fraction [38]. To imitate the same effect, drying was done under vacuum for 4 hours at 140^{o}C. The choice of drying temperature is important for flax fibres since natural fibres start degrading above 160ºC [14]. However, the debulking procedure in the CAPRI technique involves cycles of loading and unloading, whereas due to lack of proper tooling this was not feasible in our facility. Since it is expected that most of the compaction occurs during the first few cycles [38], the preform was kept under vacuum for a longer period, almost 10 hours, to compensate for the lack of cycling effect. Since after debulking, the layers are compacted and removing them can cause deformation, layers were stacked up according to their hybrid composition and were kept under vacuum as is.

No treatment was done on the natural fibres, as the epoxy used was compatible with the flax. According to Towo et al. [40], only minimal improvement is achievable by treating the sisal fibre when using epoxy as the matrix material.

3.5. Vacuum assisted resin transfer moulding process

3.5.1. Infusion setup

The VARTM setup consisted of a metallic frame, a glass mould, a vacuum chamber and a vacuum line. The glass mould was cleaned and one layer of release film was used to prevent direct contact between the resin and the mould. To further protect the glass mould from possible resin leaks under the release film, a layer of water-soluble release agent was applied.

First, the release film was cut to the correct dimensions (couple of centimeters bigger than the preform) and was placed on the mould. Then, the sealant gum was taped around the film to seal the working area. The Sealant gum was placed in a fashion to partially cover the film and the mould on three sides, and to only cover the mould on one side. This would secure the film to the mould and prevent any leakage of the resin under the film. The untapped side of the release film, allowed evacuation of trapped air between the release film and the mould. The sections of the mould under the sealant gum were carefully cleaned with Acetone to improve the adhesion.

Dried and debulked stack of fibres were placed on the release film such that 0^o fibre angle was parallel to the resin infusion direction. A peel ply was placed on the preform to prevent the laminate from sticking to the vacuum bag and infusion tubing. The porous peel ply allows resin flow through it during infusion. This property of peel ply will become more important as the next ply is applied.

Although debulking the preform prior to the infusion leads to an end product with better properties, higher compaction results in the loss of permeability and consequently making the infusion process longer [38]. This is not favorable as the epoxy resin has limited working time, and a lengthy infusion might gel the resin before fibres get fully impregnated. Therefore, a highly permeable layer, called an infusion mesh, can be placed over the peel ply to enhance the resin flow. This will change the process of infusion from in-plane to through the thickness infusion. The permeability of the preform is much lower through the thickness, since resin has to travel a much smaller distance, the overall infusion time decreases by a great factor [41]. The porous nature of the peel ply will allow the resin to flow from the infusion mesh to the fibres.

Tubing and pipe connections are the last pieces of the puzzle before applying the vacuum bag. Two spiral tubes were placed at the two ends of the preform to create a uniform resin front. Two connection ports are placed at the middle of the spiral tubes, which will connect the inlet and vent pipes inside the cavity. At the final step, everything was covered with vacuum bag and infusion pipes were installed. The position of each layer and the connections can be seen in Figure 3.2 and Figure 3.3.

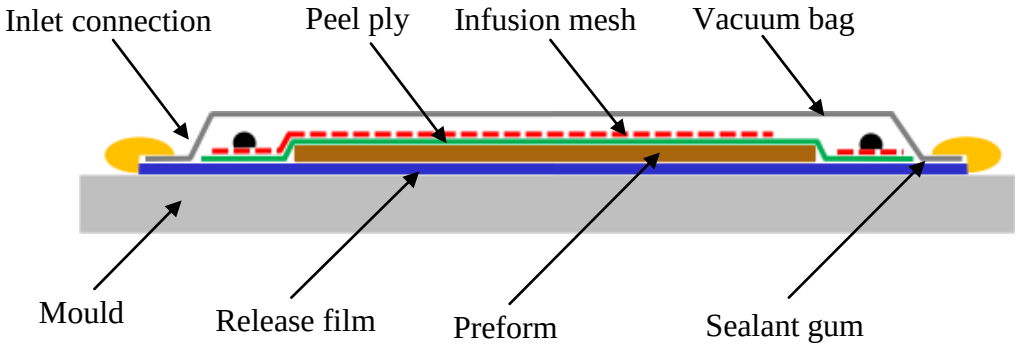

Figure 3.2 Infusion setup diagram showing different part of a VARTM setup

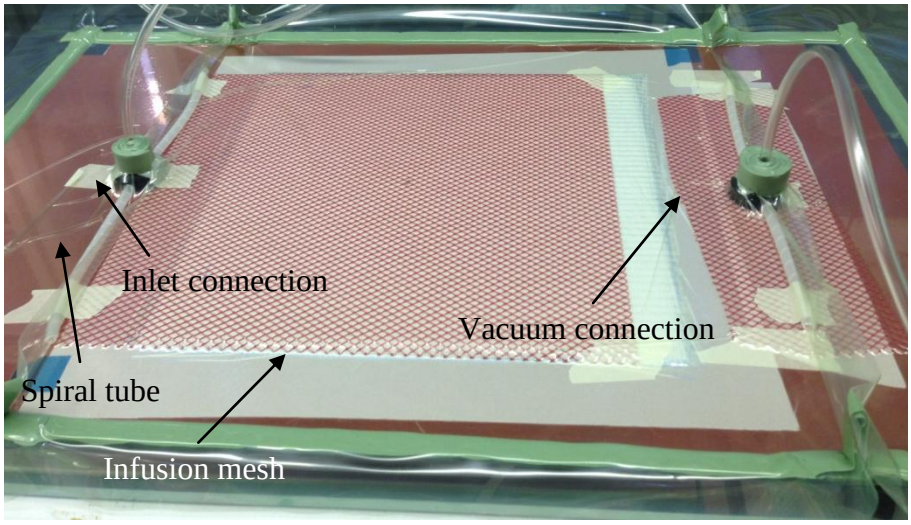

Figure 3.3 Infusion setup

3.5.2. Prefilling

Having a perfect vacuum is essential to the VARTM process, since any source of leakage can introduce voids to the preform. The room temperature curing epoxy takes 24 hours to get fully cured; thus, losing pressure during the process can cause lower compaction and hence lower fibre volume fraction. Thus, before moving on, any source of leakage had to be eliminated. The sealing quality was checked by removing the vacuum line from the cavity and monitoring the leak rate. Vacuum achievable was -98 KPa, and if there was no pressure drop detected after 30 minutes the cavity considered to be fully sealed. Afterwards, the vacuum line was connected for an hour for the second cycle of debulking.

Resin was mixed with the hardener in a proper ratio recommended by the manufacturer and it was stirred for 7 minutes in a plastic bucket. Afterwards, the mixed resin was degassed in a vacuum chamber at -98 KPa. Degassing is essential for removing any trapped air introduced to the mixture during stirring [37]. Mixture was degassed for 20 minutes, or as long as no air bubble was visible inside the epoxy. Then, the epoxy was ready for infusion.

3.5.3. Filling

The permeability has a direct relationship with compaction of the fibres [38]. Therefore, infusion at full vacuum pressure takes longer than the remaining working time of the resin after the degassing step. Reducing the vacuum pressure to -85 KPa helped to decrease the infusion time and resulted in a lower thickness gradient for the same reason as in the CAPRI process.

After setting the pressure to -85 KPa by installing a pressure valve between the vacuum chamber and the vacuum line, the inlet pipe was fully immersed inside the resin reservoir and was secured to ensure that the pipe will not escape from the bucket during the infusion. Then, the inlet was unclamped and the infusion started. Different hybrids have different permeability due to their different compositions. Since glass has higher permeability than flax, the longest infusion was observed for the 100% flax fibre laminate and the shortest for the 100% glass fibre laminate. No scientific measurement was done to fully tabulate the infusion time for the hybrid laminates, but it is evident that there is a direct relation between the amount of each fibre in the laminate and the infusion time

As mentioned earlier, using the infusion mesh changes the infusion from in-plane to through-the-thickness, and there is a difference between the permeability of the two modes. Therefore, there exists a lag between the upper and lower surface of the preform during infusion. Hammami [41] reports the same effect and gives recommendations on when to stop the infusion while using the infusion mesh. To compensate for the created lag between two surfaces of the preform, infusion mesh was cut 1 cm shorter than the preform. Thus, when resin reaches the section without the infusion mesh, the infusion goes back to in-plane mode and acts as a break to the fast infusion before it. This allowed the whole preform to be completely impregnated at the same time. Once the resin reached the end of the preform, the inlet was clamped and infusion stopped.

3.5.4. Post filling

Post-filling steps consists of bleeding and equilibrating the pressure inside the preform to reduce the thickness gradient and increase the compaction. Bleeding is a fundamental step in a VARTM process, which results in a higher volume fraction by removing the excess resin. After clamping the inlet and stopping the infusion, negative pressure was increased to -98 KPa to increase the compaction. Experience showed that leaving the vacuum source connected after clamping the inlet will cause excess bleeding and leaving dry spots. Hence, the venting tube was clamped 1 minute after clamping the inlet port. While this might not result in the best volume fraction achievable, the consistency ensured the same fibre volume fraction for hybrids with the same configuration.

After clamping the vent tube, resin still had the chance to flow from high pressure to low pressure parts and equilibrate the pressure inside the bag. It is reasonable to assume that after reaching this equilibrium there should not be any thickness gradient, but the outcome showed otherwise. The thickness variation was evident along the length of the laminate. One reason might be the limited working time left for the epoxy after finishing the infusion. It might take longer than a couple of minutes for the resin to reach an equilibrium state, while the resin gels prior to this state. Another reason can be the different compaction history along the preform. According to Robitaille [42], reinforcement compaction behaviour depends on the compaction history. This means that since the pressure was varying along the length of the laminate during the infusion, different parts of the reinforcement has experienced different compaction. Hence,

the equilibrium state does not lead to a uniform thickness. The laminate was left for 2 days under the vacuum to be fully cured.

Laminate specification Table 3.1 shows the average physical properties of all manufactured laminates. Limited control over the compaction pressure in the VARTM process resulted in thickness variation between different compositions, as flax fibres and glass fibres have different compaction rates. As a result, different fibre volume fraction was achieved for different laminates. This can be seen in Table 3.2. An indirect method for calculation of fibre content was used to assess the amount of fibre fraction (For details on this method refer to Appendix II). Because fibre volume fraction has direct influence on properties of composites [43], having similar fibre volume fraction for all compositions would have been desirable. Variable fibre volume fraction is the price to pay for ease of manufacturing, low equipment cost and low resin waste in VARTM process. Despite the mentioned dissimilarity, manufactured laminates are comparable in the context of this research since the objective is to compare the hybridization effect rather than its intensity.

Differences between densities of laminates can be seen in Table 3.1. Lighter flax fibres create laminates with lower densities compared to glass fibre laminates. However, since flax fibre laminates are thicker and contain more resin, they have higher areal density.

The amount of void content was measured using image analysis (Appendix III). Due to limited resources for sample preparations, only one sample from each composition was used to measure the void content. Consequently, reported void contents should not be interpreted as exact values. Instead, they are good indication of the quality of final parts and their integrity.

Table 3.1 Average physical properties of all compositions; standard deviations in brackets

Layup	Thickness (mm)	Areal density (g/cm^2)	Density (g/cm^3)
$[F_5]$	2.56 (3.61e-2)	3.08 (7.19e-5)	1.20 (1.24e-5)
$[F_2/G/F_2]$	2.46 (2.23e-1)	3.05 (2.64e-4)	1.24 (2.13e-5)
$[G/F_3/G]$	1.93 (6.34e-2)	2.48 (3.82e-5)	1.29 (2.42e-5)
$[G_2/F/G_2]$	1.29 (1.55e-2)	1.87 (1.01e-5)	1.45 (1.94e-5)
$[G_5]$	0.90 (1.83e-2)	1.54 (1.66e-5)	1.70 (2.94e-5)

Table 3.2 Average fibre volume fraction and void content percentage of all compositions; standard deviations in brackets

Layup	Flax fibre volume fraction (%)	Glass fibre volume fraction (%)	Total fibre volume fraction (%)	Void content (%)
$[F_5]$	31.3 (0.73)	0.0	31.3 (0.73)	0.11
$[F_2/G/F_2]$	26.2 (2.20)	3.2 (0.26)	29.4 (2.47)	0.03
$[G/F_3/G]$	24.9 (0.38)	8.1 (0.12)	33.0 (0.50)	0.01
$[G_2/F/G_2]$	12.4 (0.067)	24.3 (0.13)	36.7 (0.20)	0.01
$[G_5]$	0.0	43.3 (0.46)	43.3 (0.46)	0.05

3.6. Coupon preparation

Cured laminates were cut into rectangular 25 x 2.5 cm coupons, which is according to the ASTM standard D3479 [44]. Coupons were cut perpendicular to the infusion direction to prevent thickness variation within a single coupon. Since flax fibres are very sensitive to water, a band saw was used to cut the coupons from the flax fibre preforms. For hybrid laminates and the glass fibre laminate this was not possible since using a band saw would have caused pull out of glass fibres. Hence, a wet saw with a diamond blade was used. Great care was taken to use as little water as possible, and coupons were dried right after they were cut to prevent any swelling of the flax fibres. All samples were polished using fine sanding paper to eliminate any edge effect and

any stress concentration created during cutting. The ASTM recommendation is to sand to the point that fibres will be visible from the sides of the sample.

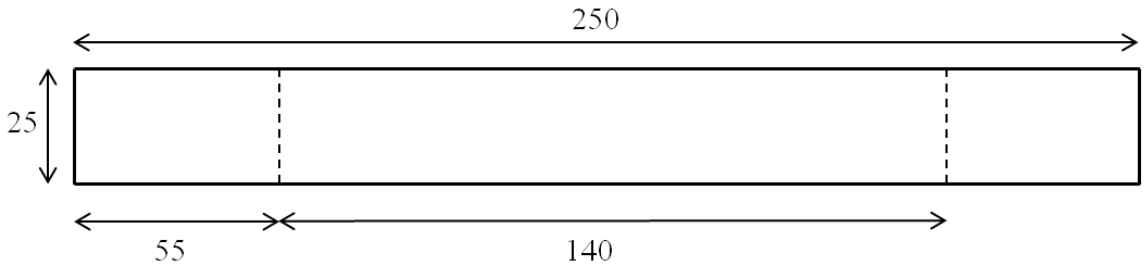

Figure 3.4 Dimension of coupons (in mm) used for experiments

3.7. Testing method

3.7.1. Quasi-Static Test

All tests were done according to ASTM D3039 standard [45] for tensile test and D3479 standard [44] for tension-tension fatigue tests. For quasi-static tests, 5 random samples were tested. The force applied on the specimen was measured using the load cell sensor of the machine, and for strain measurement a 1-inch extensometer was utilized. While it is not necessary to use tabs for testing cross ply laminates, an abrasive mesh was used to eliminate any slippage of specimen inside the grips. Consistent gage area failure was observed for all specimens. Coupons were loaded with the rate of 0.01 mm/s up to total fracture and data extracted from each test was used to draw the corresponding stress strain curve.

3.7.2. Tension-tension fatigue test

As for the fatigue tests, the same pressure and abrasive mesh was used to grip the samples. First, the samples were loaded gradually until the desired load peak, and then the cyclic load was followed according to the appropriate loading frequency and loading ratio. Each composition was tested at three peak loads, 80%, 65% and 50% of its ultimate strength. Four samples were tested at each load level. All samples were tested at stress ratio R = 0.1, which indicates the ratio between the high and low peaks of loading (Equation 3.1). Three different testing frequencies were used. At 80% loading level since the difference between the two peaks was high, tests were

conducted at 1 Hz frequency to enable the machine to properly follow the loading profile. At lower loading levels higher frequencies were used for convenience, since large number of cycles was expected. Thus, for 65% and 50%, 1.5 Hz and 3 Hz were used. The samples were kept under cyclic loading until total fracture was achieved.

$$R = \frac{\sigma_{min}}{\sigma_{max}}$$ Equation 3.1

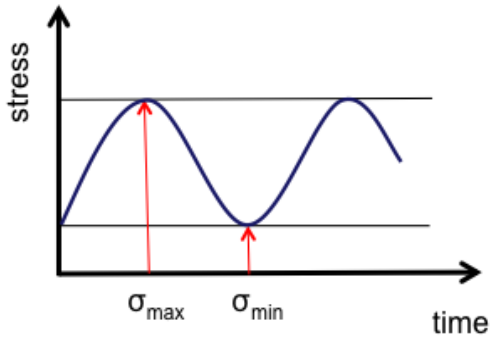

Figure 3.5 Diagram showing cyclic load. Positive σ_{max} and σ_{min} defines the fatigue to be tension-tension

4. Results

This chapter aims to present the results carried out from the monotonic and cyclic tests. In the first section, the results of quasi-static tests are presented to assess the strength and static properties of the laminates under study. With this information in hand, the second section presents the fatigue tests conducted along with the respective results. This is followed by the modulus evolution of composite laminates, which is related to the damage mechanism of each hybrid or non-hybrid composition. Finally, the chapter is concluded by the study of fractured surface.

4.1. Quasi-static results

Representative loading curves of all laminates are presented in Figure 4.1, and the detailed data for all configurations are summarized in Table 4.1. When looking at these values, note that there is a noticeable difference between the strain-to-failure of the flax fibre laminates and the glass fibre laminates. Strain compatibility of the fibres used in a hybrid laminate influences the degree of agreement between the actual experimental data and the predicted values using a rule-of-mixtures [23]. Since the hybrids studied in this research are constructed with fibres that are different in their failure strain by a large factor, a significant deviation from the rule-of-mixtures is expected. From Table 4.1, note that while the actual strength deviates largely from the rule-of-mixtures, the longitudinal modulus is in a good agreement. It is generally accepted that tensile modulus in the 1-direction obeys the rule-of-mixtures [46]. This is explainable by the nature of the modulus, which is the ratio of the change caused by the stress to the original state of the material. Since both fibres are elongating at the same rate and the modulus is measured between 0.1% and 0.3% strains, before any fibre fracture, the rate of the change will project its consecutive inherited properties from each material according to mixture ratio.

The strength of hybrid composites is governed by the lowest strain-to-failure fibres in that laminate [46]. However, there is always a positive hybrid effect, which is defined as an increase of the overall strain and the strength of the composite laminate compared to the amount constrained by the low strain-to-failure fibres, or the flax fibres in the context of this research. The bridging of high elongation fibres after the breakage of low strain fibres causes this effect, which is so called the hybrid effect. In a non-hybrid laminate, the stress concentration caused by

the fibre fracture results the total failure of the sample. Whereas in a hybrid laminate, if the higher strain-to-failure fibres can carry the load after the breakage of the lower strain-to-failure fibres, the load then gets redistributed causing the pseudo yielding effect. Good adhesion between the two different fibres and the resin system results in a better hybrid effect, as after the breakage of the low elongation fibres, the high elongation fibres transfer the stress back to them [46]. This was not the case in any of the hybrids studied. While flax showed good compatibility with the epoxy, delamination between flax and glass layers was evident at the fracture cross sections.

From Figure 4.1, it is apparent that the static properties of all hybrid laminates are bounded by the single-fibre composite properties, the lower bound being the flax fibre laminate and the upper limit being the glass fibre laminate. This shows that for static properties, hybrids cannot surpass their inherent properties.

Table 4.1 Mechanical properties of all laminates; standard deviation is shown in brackets

Composition	**Experimental Ultimate Strength (MPa)**	**Rule of Mixtures Prediction (MPa)**	**Experimental Modulus[1] (GPa)**	**Rule of Mixtures Prediction (MPa)**
$[F_5]$	112.24 (2.08)	112.24	12.16 (1.68)	12.16
$[F_2/G/F_2]$	113.02 (7.59)	124.42	12.41 (0.82)	12.75
$[G/F_3/G]$	138.98 (3.67)	168.08	13.20 (1.52)	13.83
$[G_2/F/G_2]$	254.67 (6.46)	280.02	17.37 (0.77)	17.24
$[G_5]$	419.71 (12.07)	419.71	22.13 (1.1)	22.13

[1] Tensile modulus of elasticity has been calculated using $E = \frac{\Delta\sigma}{\Delta\epsilon}$ with considering the absolute strain range of 0.001 to 0.003 according to Table 3 of ASTM D3039M standard.

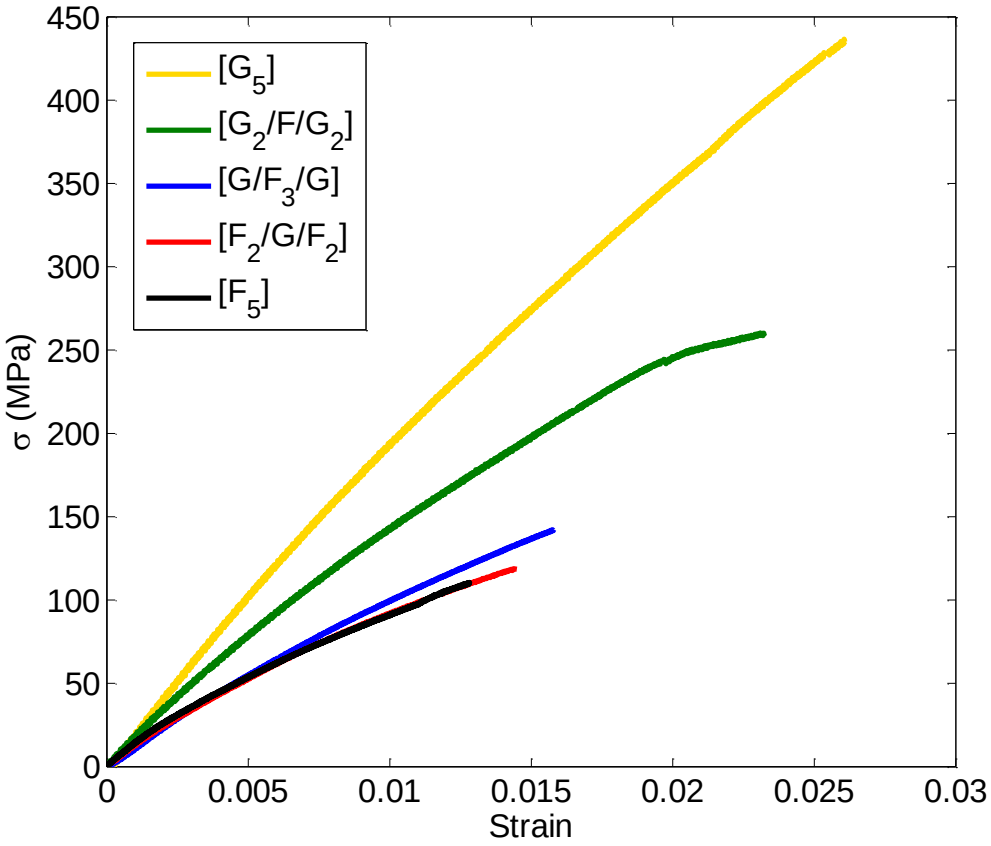

Figure 4.1 Stress-Strain Curves for all laminates. The legend shows each configuration in which [F] stands for "Flax Fabric" and [G] stands for "Glass Fabric"

4.2. Fatigue test results

Data collected from fatigue tests were used to create the S-N curves for each type of composite configuration. Figure 4.2 shows the S-N curve corresponding to the non-hybrid flax laminate, where the x-axis shows the number of cycles on a logarithmic scale and the y-axis corresponds to the maximum applied stress of the fatigue cycle, in MPa. Dots on the graph represent the actual data extracted from the tests at three different loading levels. The use of linear curve fitting was possible based on two basic assumptions: one being the linear distribution of data on a logarithm scale, and the other is that the variance of the log life is constant throughout the entire range of the tests. Thus, a simple linear curve fit, as shown in Equation 4.1 was constructed using directives from ASTM standard E739-10 [47]. In Equation 4.1, A and B are fitting parameters and Y and X are dependent and independent variables respectively. More details on the construction of the S-N curve are in Appendix IV.

$$Y = A + BX \qquad \text{Equation 4.1}$$

The adequacy of the linear assumption was checked using statistical tests for linearity. For detailed methods and calculated values, refer to Appendix VI.

Confidence bands, which are noted on the graph by dashed lines, were constructed based on a t-distribution 95% confidence interval. They are an indication of data scatter and an important parameter while looking at a material's fatigue life for design purposes. Details on construction of confidence band can be found in Appendix V. S-N curves for all tested compositions are presented in Appendix VII.

Table 4.2 shows the standard deviation corresponding to each tested laminate. As mentioned above, the assumption is that the standard deviation is constant throughout the entire tested range. The standard deviation has been calculated based on Equation 4.2 as the square root of variance.

$$\hat{\sigma} = \sqrt{\frac{\sum_{i=1}^{k}\left(Y_i - \hat{Y}_i\right)^2}{k-2}} \qquad \text{Equation 4.2}$$

The standard deviation of the data is based on the logarithm of the fatigue life and it is an indication of the scatter of data in the entire range of tested samples at three different load levels. Higher standard deviation values for non-hybrid FFRE compare to non-hybrid GFRE shows the inconsistency of the flax material and the variability in their properties. Comparing the standard deviations, the highest value belongs to the [F_2/G/F_2] laminate, which is due to an unintentional error in the manufacturing step. Two different batches manufactured in this composition were inconsistent in their amount of resin, causing a different fibre volume fractions for each batch. Due to the lack of sufficient raw material, the decision was made to conduct the tests with already manufactured samples. Despite the existing differences, fatigue data was useable and the scatter of data was within the acceptable statistical range according to replication factor and linearity adequacy. For two other hybrids namely [G/F_3/G] and [G_2/F/G_2], their corresponding standard deviation is lower than in a non-hybrid FFRE laminate, indicating slight remedy for the inconsistency of flax material by hybridization with glass fibres.

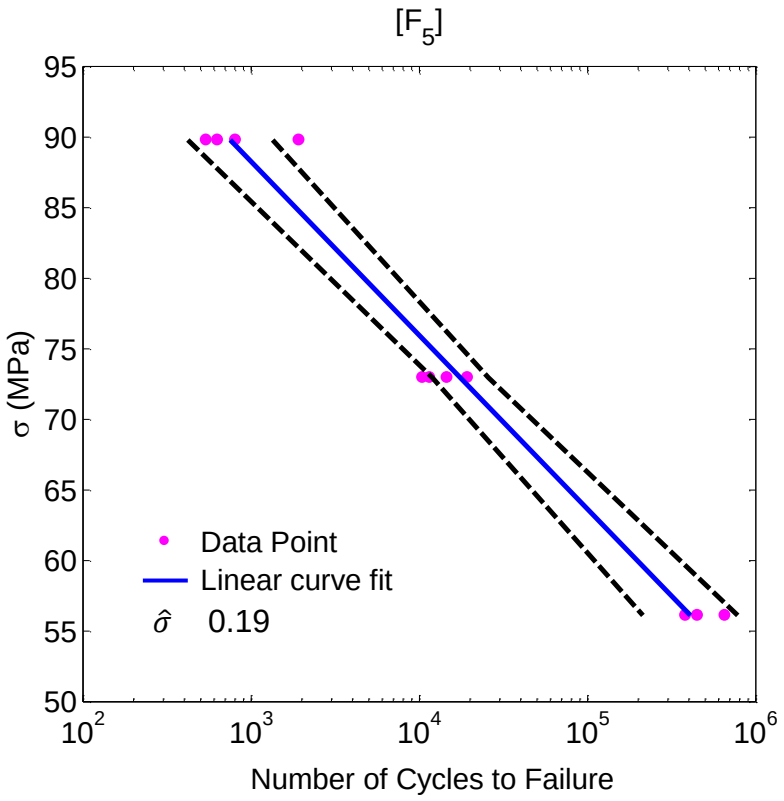

Figure 4.2 S-N curve corresponding to the [F_5] laminate

Table 4.2 Standard deviation (SD) of entire fatigue life, on a logarithmic scale

Layup	SD (Log N)
$[F_5]$	0.19
$[F_2/G/F_2]$	0.26
$[G/F_3/G]$	0.16
$[G_2/F/G_2]$	0.17
$[G_5]$	0.12

Figure 4.3 through Figure 4.5 shows S-N curve compilation of all laminates. In Figure 4.3, the y-axis is the absolute stress applied to specimens, and for Figure 4.4 and Figure 4.5, the y-axes are normalized based on the density and the strength respectively. The x-axis in all graphs is the number of cycles to failure on a logarithmic scale.

4.2.1. Absolute S-N curves

Starting from Figure 4.3, it can be seen that as the $[G_5]$ specimen inherits better fatigue strength from its superior static properties, it can withstand more load compared to other laminates for the same number of cycles. This is shown as the $[G_5]$ S-N curve lays above all other S-N curves. The $[G_2/F/G_2]$ hybrid laminate's S-N curve lies lower than the plain glass fibre laminate and higher than other laminates. While its fatigue strength is lower than the $[G_5]$ specimen, it has better fatigue life in terms of total number of cycles it can withstand. Looking at the $[F_2/G/F_2]$ and $[G/F_3/G]$ laminates' S-N curves compared to the one for plain flax fibre composite, there is an overall improvement of fatigue strength. This means that for the same number of cycles to failure, the mentioned hybrids can withstand more load due to introduction of stronger fibres to the laminate. For instance in Figure 4.3, at the 800 cycles, $[F_2/G/F_2]$ and $[G/F_3/G]$ laminates have 0.69% and 23.8% higher load peak compared to the $[F_5]$ laminate.

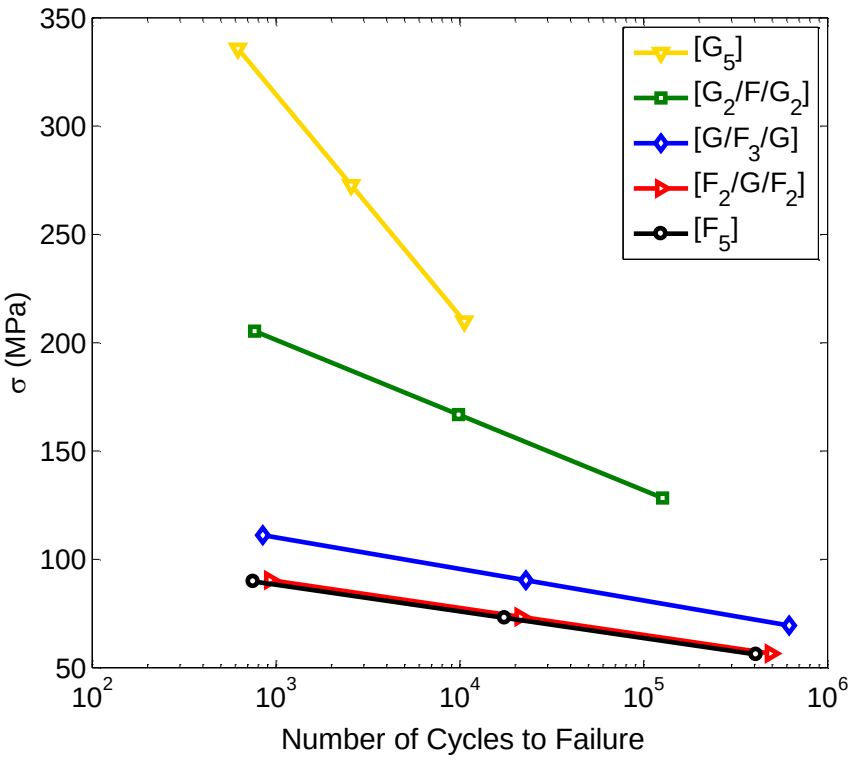

Figure 4.3 Compilation of S-N curves for all composition in terms of absolute stress levels

4.2.2. Specific (weight-normalized) S-N curves

To observe the performance of each material based on their weight, S-N curves were normalized based on the density of each laminate. Figure 4.4 shows the compilation of all normalized S-N curves. While the general trend is similar to the previous case, here the gap between the non-hybrid GFRE and [G_2/F/G_2] hybrid laminate has diminished significantly. This is due to the lower density of the hybrid laminate after the replacement of a glass fibre layer with a lighter flax fibre fabric. A study done by Liang et al. [33] on fatigue behaviour of flax/epoxy and glass/epoxy composites shows the same fatigue behaviour for glass fibre composite as the non-hybrid glass laminate studied in this research. In addition to the studied loading range in this research, Liang et al. tested samples at lower loading levels. Using the data from mentioned study, the S-N curve for the glass/epoxy laminate was extended up to the available data, which can be seen as a black dashed line in Figure 4.4. This was of course possible by the linear fatigue

behaviour of glass fibres at those loading levels. Referring to the dashed line, at specific stresses less than 110 MPa $(g/cm^3)^{-1}$, the hybrid laminate outperforms the plain GFRE laminate. The difference gets bigger as the specific stress decreases. For the data available at the lowest specific load at 90 MPa $(g/cm^3)^{-1}$, the $[G_2/F/G_2]$ hybrid laminate withstands 160 x 10^3 more cycles compared to non-hybrid glass fibre laminate. Looking at the lower part of the chart in Figure 4.4, the non-hybrid FFRE has minor fatigue strength advantage over $[F_2/G/F_2]$ hybrid laminate due to its lower density. For the other flax fibre dominant hybrid, namely $[G/F_3/G]$, the hybrid laminate still maintains the upper hand position despite its higher density. The density of each composition has been repeated in Table 4.3.

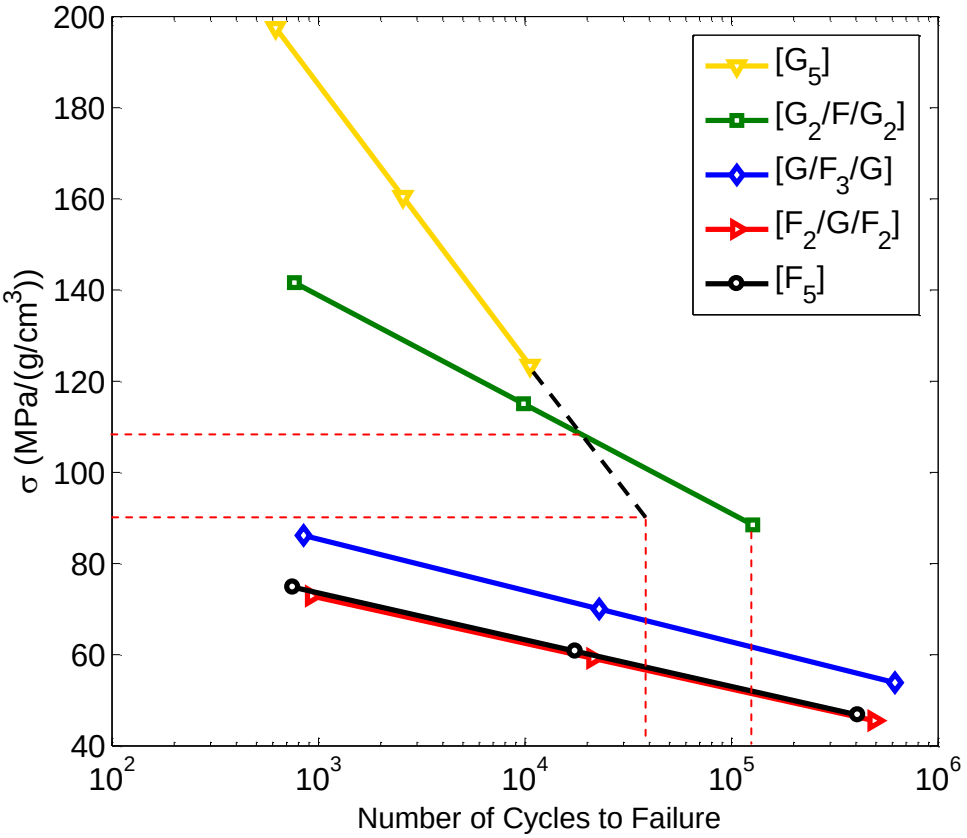

Figure 4.4 Compilation of density normalized S-N curves for all compositions

Table 4.3 Density of laminates, standard deviations in brackets

Layup	Density (g/cm^3)
[F_5]	1.20 (1.24e-5)
[F_2/G/F_2]	2.13 (2.13e-5)
[G/F_3/G]	2.42 (2.42e-5)
[G_2/F/G_2]	1.94 (1.94e-5)
[G_5]	2.94 (2.94e-5)

4.2.3. Strength normalized S-N curves

Figure 4.5 shows fatigue curves for all compositions normalized by the tensile strength. The slope of each line defines the fatigue sensitivity, which is an indication of the fatigue performance of a material as the cycling stress level changes [31]. Table 4.4 contains the absolute value of each S-N curve slope. The importance of fatigue sensitivity becomes more apparent as the imposed cyclic stress decreases. By comparing the fatigue sensitivity coefficient of each laminate from Table 4.4, it reveals that flax fibres exhibit improved performance over glass fibres in the tested region. This is in accordance with Table 4.5 that shows the average number of cycles to failure of compositions at normalized loading levels. It can be seen that non-hybrid FFRE outperforms glass fibre composites in low load bearing applications as it can take more cycles prior to failure for the same amount of normalized stress compared to non-hybrid GFRE.

Comparing the non-hybrid GFRE laminate with the hybrid laminate where a layer of glass fibre has been replaced with flax material, namely the [G_2/F/G_2] laminate, the overall fatigue sensitivity is lower. However, this improvement is not without a cost. Lower fatigue strength of the mentioned hybrid limits the performance of mentioned hybrid laminate. Looking at non-hybrid FFRE and its dominant hybrid laminate [F_2/G/F_2], the effect of replacing the flax fibres with glass fibres is negligible. Unexpectedly, the [G/F_3/G] composition has the lowest fatigue sensitivity coefficient despite having two layers of glass fibres. While there has been no exclusive study in this research on the position of fabrics in a hybrid laminate, this observation can suggest that having glass fibres at the outer layer results in the best outcome.

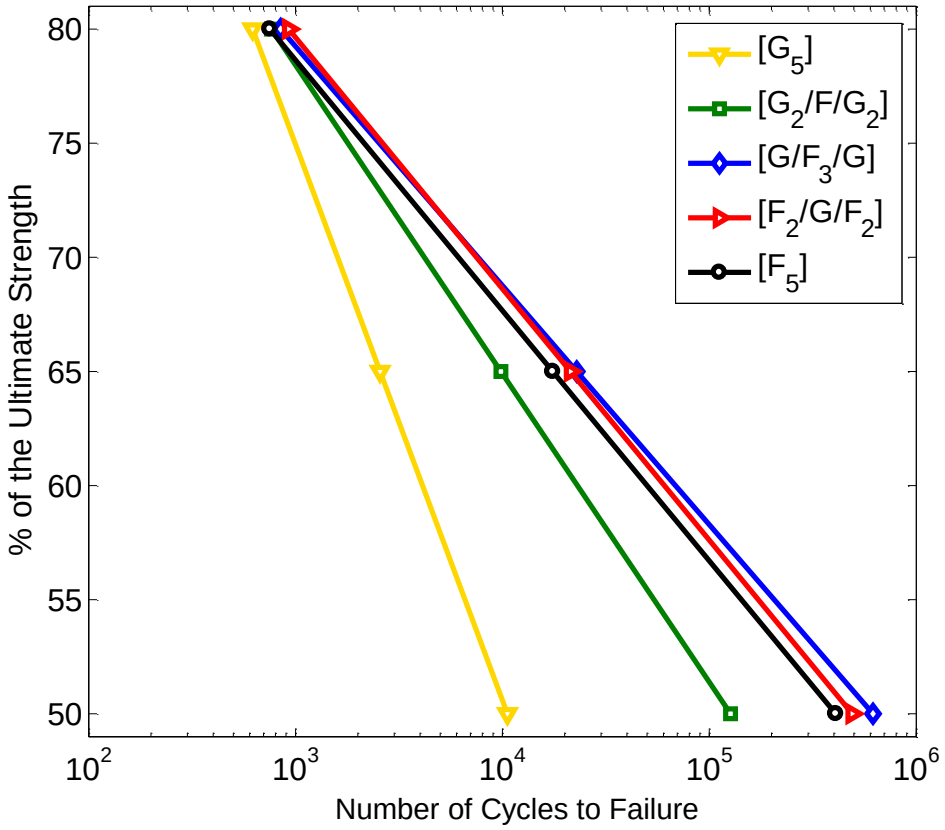

Figure 4.5 Compilation of strength normalized S-N curves for all compositions

Table 4.4 Fatigue sensitivity of compositions

Layup	**Fatigue sensitivity coefficient**
$[F_5]$	0.04875
$[F_2/G/F_2]$	0.04894
$[G/F_3/G]$	0.04657
$[G_2/F/G_2]$	0.06008
$[G_5]$	0.10828

Table 4.5 Average fatigue life of all specimens; standard deviations in brackets

	80 % UTS		**65 % UTS**		**50 % UTS**	
	N_{avg}	Log (N_{avg})	N_{avg}	Log (N_{avg})	N_{avg}	Log (N_{avg})
[F_5]	977 (644)	2.93 (0.25)	13986 (3947)	4.13 (0.12)	496688 (142445)	5.68 (0.12)
[F_2/G/F_2]	1341 (890)	3.07 (0.24)	13917 (5149)	4.12 (0.15)	708719 (392349)	5.79 (0.26)
[G/F_3/G]	912 (71)	2.96 (0.03)	21335 (10260)	4.30 (0.18)	730441 (355701)	5.82 (0.22)
[G_2/F/G_2]	712 (224)	2.84 (0.14)	12617 (3583)	4.09 (0.12)	127178 (77530)	5.06 (0.23)
[G_5]	696 (249)	2.82 (0.15)	2318 (777)	3.35 (0.14)	11402 (1398)	4.05 (0.05)

4.3. Modulus evolution

The evolution of specimen's modulus reveals information on the damage progression of the material as it is subjected to fatigue loading. Monitoring the modulus variation during the cyclic loading can give the user clues on how the material behaves at a specific time during its fatigue life.

4.3.1. Modulus evolution theory

The basic idea behind the modulus decay is to monitor the ratio of the modulus at each cycle normalized to the modulus of the first cycle. This ratio is thus independent of the specimen's cross-sectional area and its initial length, as they are assumed to remain constant during fatigue loading. Hence, the modulus at each cycle can be replaced by the ratio of the load difference over the changes of the head position as described in Equation 4.3. Using the machine's head position as an indication of the strain is a reasonable assumption when there is no slippage of the

specimen inside the grips. Utilizing abrasive cloth and enough grip pressure assured no slip condition at the grips. Furthermore, using head position in modulus decay monitoring is advantageous since it can reflect all changes at the entire gage section.

$$E_i = \frac{(F_i^{max} - F_i^{min})/(d_i^{max} - d_i^{min})}{(F_o^{max} - F_o^{min})/(d_o^{max} - d_o^{min})} \qquad \text{Equation 4.3}$$

Here, *F* stands for the force applied to the specimen and *d* denotes the head position. The subscript '*i*' indicates the i^{th} cycle and subscript '*o*' stands for the first cycle. Superscripts *max* and *min* indicates the maximum and minimum value of each parameter during a cycle.

4.3.2. Modulus evolution evaluation

Figure 4.6 through Figure 4.8 show the modulus decay of samples at three different loading levels. Each graph corresponds to one normalized stress level. Modulus decay of all samples was monitored, and for the same stress level, similar behaviour was observed for repeat tests of the identical compositions, with less than 5% difference. Due to the noisy nature of the raw data, the most clear data was chosen to represent its population. Hence, each line on the graphs represents the modulus evolution of a single sample.

Looking at the 80% loading level modulus decay in Figure 4.6, non-hybrid flax fibre laminates and non-hybrid glass fibre laminates have two different behaviours. GFRE laminate's modulus decreases within three steps similar to traditional composites under fatigue loading. As described by Naik [28], reduction in modulus in woven fabric takes place in three stages. First, there is a steep decrease in the modulus due to the formation of matrix micro cracks and transverse failure of the weft fibres. As the micro cracks become saturated, the decay of modulus slows down and next damage mechanism starts. Matrix cracks in the resin rich regions and shear failure of warp fibres characterizes the second stage of modulus evolution. As the cycles progress further, damage accumulates in fibre and matrix regions, and coupling between different damage modes and cracks causes delimitation and more acute stress concentrations. The last stage is characterized by another rapid decay in modulus caused by the wrap strand failures and thus causing the total fracture of the sample. Since calculating the modulus decay with head position data from the machine created a noisy outcome, the last step has not been captured in Figure 4.6.

In contrast, FFRE laminates show an increase in the modulus at early stages, known as the stiffening effect. Then, the modulus starts decreasing at a very slow rate, where it can also be considered as becoming constant. The stiffening effect has been reported for synthetic fibre composites caused by annealing effect of the polymer matrix [48]. However, since the resin system used in all laminates was the same and the stiffening effect has only been observed in laminates with significant amount of flax fibres, this phenomenon should have roots in the fibres rather than in the matrix. Baley [49] reports 60 to 80% increase in Young's modulus of flax fibres when loading axially. He explains this increase as the cellulose microfibrils wounded spirally with a certain winding angle, become straight after applying the load resulting in the increase of the stiffness of the fibres. The stiffening effect is less prominent in a flax fibre laminate since epoxy resin will limit this effect. Re-orientation of the misaligned fibres in the visco-elastic matrix under tensile load, and reduction of the crimp in the woven fabric are other reasons casing stiffening effect [28]. The [F_2/G/F_2] and [G/F_3/G] hybrid laminates do not show any stiffening effect, but the modulus decay behaviour is close to the one for non-hybrid flax fibre laminate with insignificant amount of modulus reduction. Hence, in the case of flax dominant hybrids, the modulus reduction is controlled by the by flax fibres.

Unlike the two other hybrids, [G_2/F/G_2] laminates have more severe modulus reduction than plain glass fibre laminates. This decrease in the modulus is explainable by looking at the strain-to-failure difference of the fibres used in studied hybrids. Since the [G_2/F/G_2] laminate is a glass dominant hybrid, the amount of strain is being dictated by the glass fibres, which is much higher than the strain that flax fibres can withstand. Consequently, during the fatigue loading at high stress levels, flax fibres disintegrate within the laminate causing further decay in the modulus.

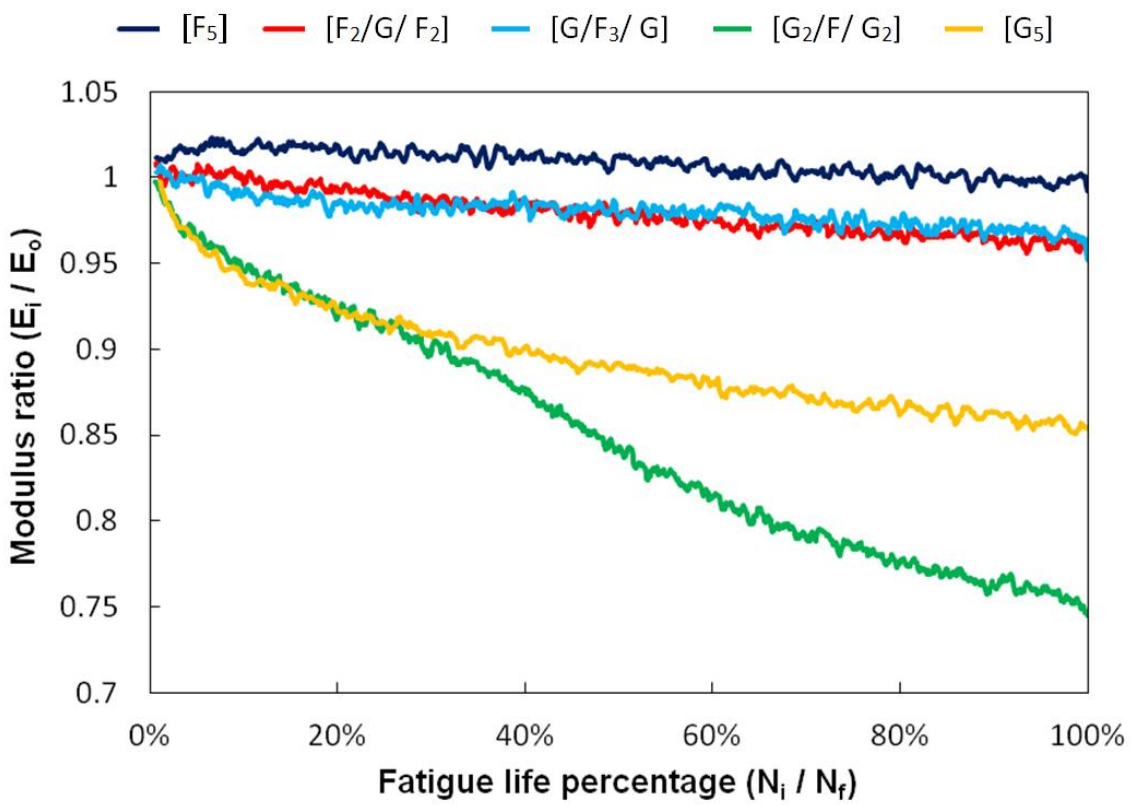

Figure 4.6 Modulus decay of specimens tested under 80% loading level

Comparing the graphs at different loading levels reveals that there is more decay in modulus at lower stress levels. For instance, the final normalized modulus for $[G_5]$ laminate from high to low stress levels are 0.87, 0.84 and 0.80 respectively. This is expected since as Shokrieh [28] explains, failure of the specimen under cyclic load takes place when the stiffness is reduced to a critical level. At lower stress levels, the critical value for stiffness is lower. Hence, more reduction in the modulus is possible as the specimen goes through more cycles.

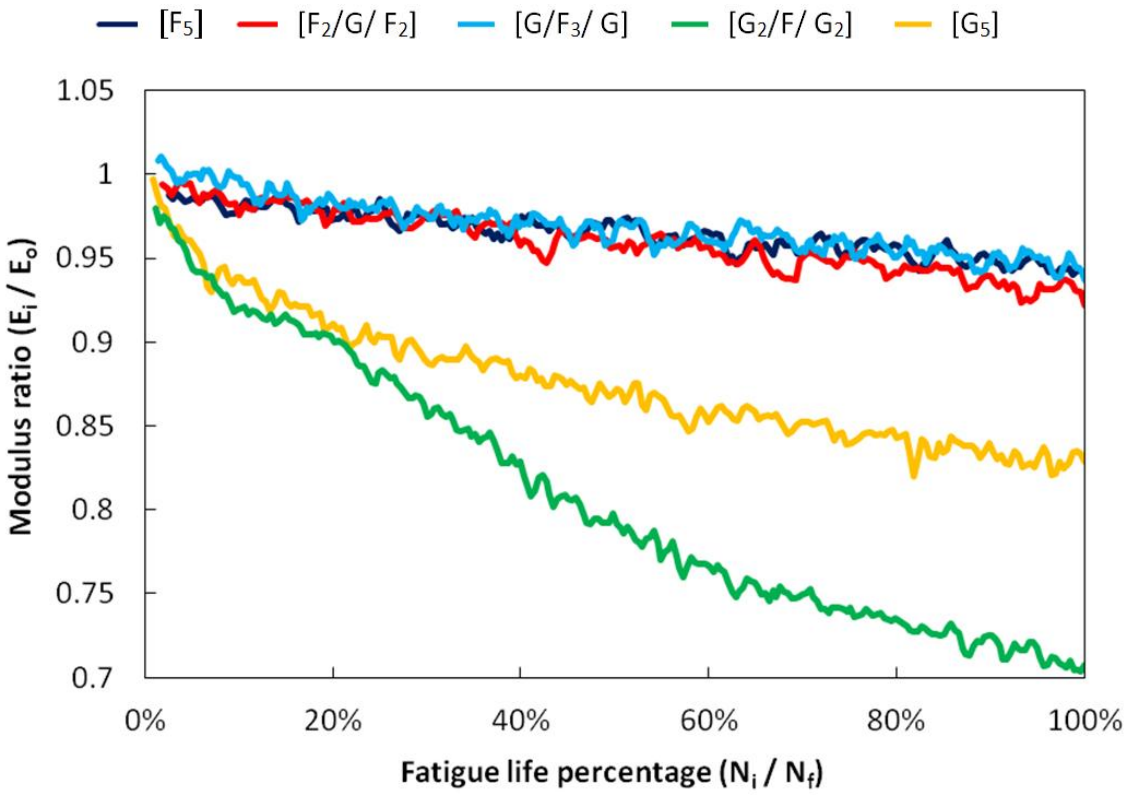

Figure 4.7 Modulus decay of specimens tested under 65% loading level

While at 65% stress level the modulus decay of all compositions is relatively similar to the 80% stress level, looking at Figure 4.8 for the 50% stress level, one can see a different behaviour in the [G_2/F/G_2] hybrid laminate. In this case, the initial rapid reduction of the modulus is analogous to previous cases, which indicates that the damage mechanism is still dominated by the glass fibres. However, this rapid reduction occurs at an earlier stage compared to the non-hybrid GFRE laminate, which is due to the existence of the flax fibres in the hybrid laminate. Here, as shown in Figure 4.8, as the stress level is lower, the amount of strain is within the tolerable range of flax fibres' strain. Thus, flax material has the chance to show its potential. It is expected to see lower modulus reduction in [G_2/F/G_2] hybrids at lower loading levels than what has been tested in this research, which is in accordance with Figure 4.4. Here the mentioned hybrid laminate outperforms the non-hybrid glass fibre laminate at lower normalized stress levels.

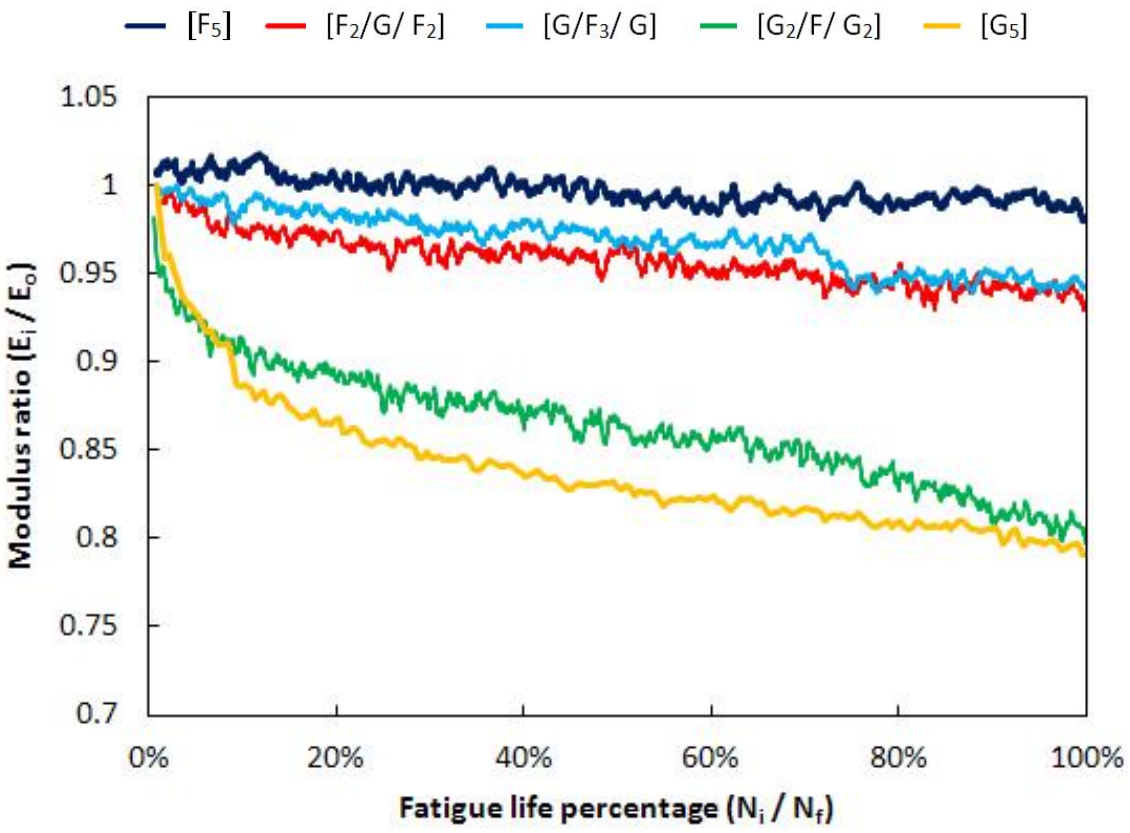

Figure 4.8 Modulus decay of specimens tested under 50% loading level

4.4. Study of fracture

Failure under fatigue loading in composite materials is complicated to analyze as there are many modes contributing to the failure. Recognizing the contributing factors after the fracture requires special tools and knowledge about each damage mechanism and their effect. In previous section, damage mechanisms and their intensity were studied by monitoring the modulus evolution at each composite composition. In this section the attempt is to study the post fatigue fracture specimens to first recognize the sources causing the failure, and secondly to distinguish the difference between the failures of different compositions.

Figure 4.9 shows the fracture surface of [G_2/F/G_2] hybrid laminate at three different loading levels. As mentioned earlier, the general damage generation sequence in composite laminates made out of woven fabrics starts from intralaminar and interlaminar matrix cracks mostly in transverse direction followed by delamination due to the coupling of the cracks. Then, the shear failure of longitudinal fibres creates enough stress concentration at which the applied stress exceeds the residual load-carrying capability of the specimen; it is then that the final fracture takes place [17]. Due to the transparency of glass fibres, the flax fabric located at the middle section is visible. Moreover, localized matrix cracks are visible from the surface indicated by the white spots on the specimen. As can be seen from Figure 4.9, matrix cracks are localized, as woven bundles tend to trap the cracks and prevent them from propagating [28].

When comparing the fracture surface at different loading levels, the fracture mechanism is closer to static failure at high stress levels and is characterized by sudden fibre fracture. This leads to releasing of high amount of energy and causing total matrix failure close to the fractured region. Total matrix failure is indicated by total separation of the glass layers from the flax layer at the fractured region as shown in Figure 4.9 (a). As the stress level decreases, the fracture becomes more gradual allowing other damage mechanisms to grow further. Consequently, looking at Figure 4.9 (c), which shows the fractured surface of the specimen tested at 50% stress level, more localized matrix cracks over the entire specimen's gage length are observed as compared to specimens tested at 80% stress level. Moreover, the fracture is less catastrophic, thus leading to a cleaner fracture surface. The fracture section of 65% stress level, shown in Figure 4.9 (b), exhibits some fibre pull out which is an indication of insufficient matrix to fibre adhesion.

(a) (b) (c)

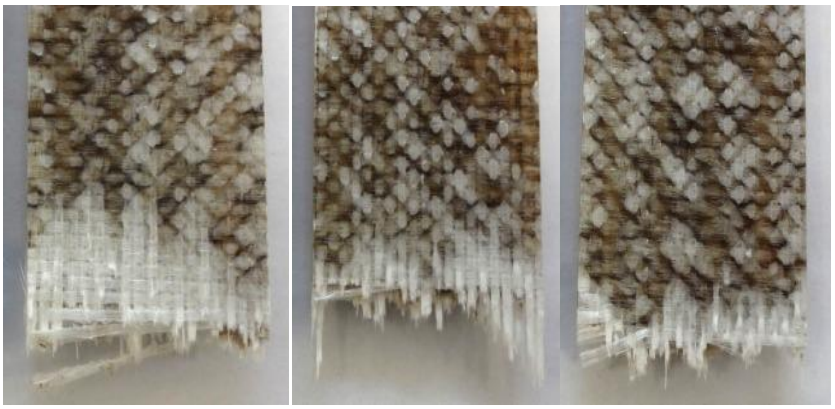

Figure 4.9 Fracture region of [G_2/F/G_2] specimens tested at different stress levels. (a) 80% loading level, (b) 65% loading level, (c) 50% loading level

The general damage mechanism is similar for other laminate compositions as well. As for the difference between the fractures at different stress levels, the trend is also analogous to what has explained above. However, there are subtle differences in terms of visibility of the cracks and their form. Localized transverse matrix cracks under cyclic load are apparent in Figure 4.10 (a) and (b) where flax fibres are placed at the outer layers. The delamination that occurred in the case of [G_2/F/G_2] hybrid laminate at 80% loading level does not exist in non-hybrid laminates, which can be seen from Figure 4.10 (a) and (e). This is an indication of the bad adhesion between flax fibres and glass fibres. In the case of hybrid laminate [F_2/G/F_2], Figure 4.10 (b), while there is no indication of delamination at the fracture region, glass fibres have been pulled out from the other side of the specimen which suggests the inadequate adhesion between two fibres.

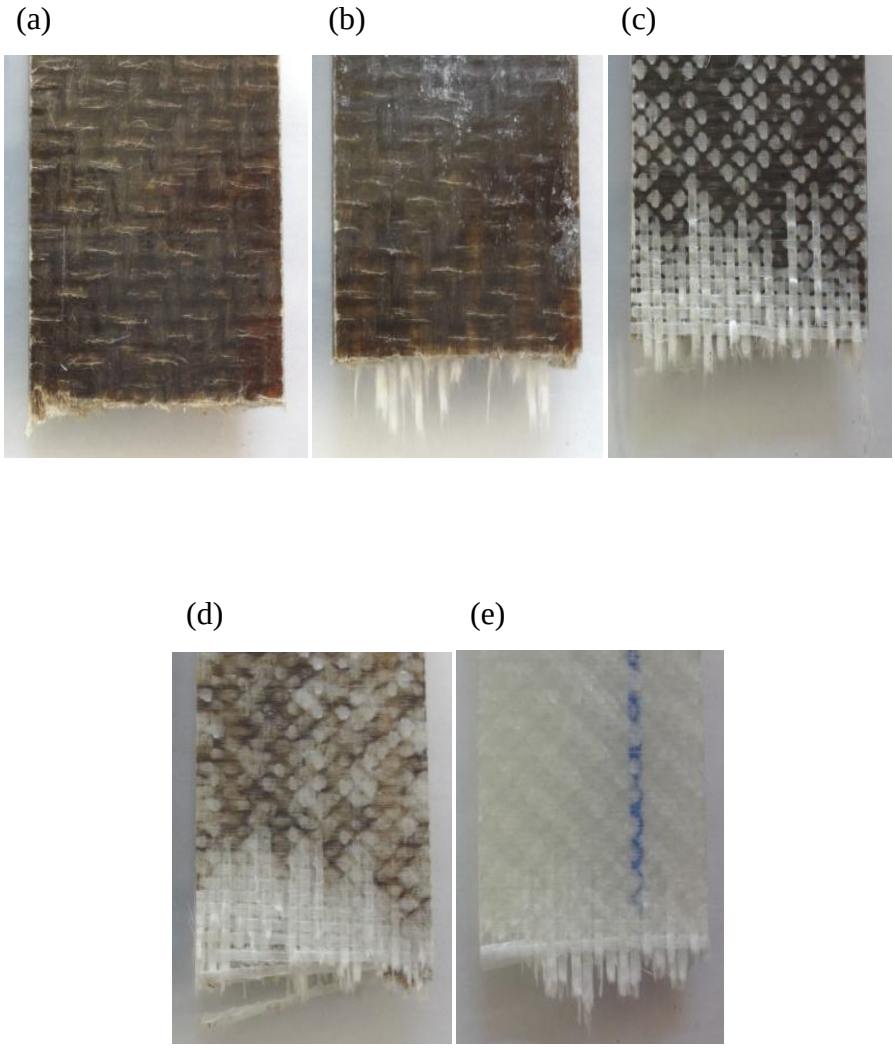

Figure 4.10 Fracture region of all composition for specimens tested under 80% stress level. (a) [F_5], (b) [F_2/G/F_2], (c) [G/F_3/G], (d) [G_2/F/G_2] and (e) [G_5]

5. Discussion

Looking back at the results and the correlation between them, several observations can be drawn regarding the objectives of this research. For investigating the effect of hybridization between glass fibres and flax fibres, making statements based on one set of results can be misleading and unreliable. In this section the aim is to treat all results as one entity and discuss the effect of hybridization, its potential and limitations.

Introducing flax fibres in a glass fibre laminate results in drastic changes in the performance of the composite laminate, as was seen in the case of the [G_2/F/G_2] hybrid laminate. Drops in the static strength and as a result, a decrease in the fatigue strength of the laminate are the first noticeable effects. Nevertheless, the hybrid laminate benefits from better fatigue stability than that exhibited by glass fibres alone. Lowering the fatigue sensitivity is a direct result of introducing flax fibres to the laminate. Enhancement in fatigue sensitivity means increase in the number of cycles to failure, particularly at low fatigue loadings. The hybrid laminate also benefits from the low density of flax fibres. Combination of lower fatigue sensitivity and lower density of [G_2/F/G_2] hybrid laminate compared to non-hybrid GFRE, results in a better fatigue strength for the hybrid laminate after certain load (Figure 4.4). Looking at the modulus decay charts, one can observe that damage formation in this type of hybrid is sensitive to the amount of strain at which the laminate is performing. At high stress levels, the disintegration of flax fibres cause more intense stiffness reduction, whereas at low stresses hence low strain levels the modulus reduction is slighter than the non-hybrid laminate.

This set of results emphasizes the importance of strain compatibility between the fibres in a hybrid laminate. Consequently, in a hybrid laminate where high strain-to-failure fibres are dominant in volume fraction, the laminate performance is limited by the low strain-to-failure fibres. Obeying the strain limitation allows the hybrid laminate to benefit from both types of fibres. Other advantages of flax fibres including high damping properties and sound abatement capabilities can promote better use for these types of hybrids, such as durable interior panels for aircrafts, trains and automobiles [18], [11].

In the case of flax dominant laminates ([F_2/G/F_2] and [G/F_3/G]), the changes are more subtle. In contrast to the previous case, replacement of a layer of flax fibre with glass fibre does not result

in a great change of properties compared to non-hybrid FFRE. Since stronger fibres (glass fibres) have higher strain-to-failure, the dominant low strain-to-failure fibres limit the performance of stronger fibres as their full potential is achieved when they are fully stretched. Some changes start to appear as the amount of glass fibre content increases as in [G/F_3/G] hybrid laminate. In this case, the hybrid laminate has higher static and fatigue strength while it benefits from the fatigue stability of flax fibres. Negligible modulus reduction in all fatigue loadings is an indication of this behaviour. Moreover, lower fatigue sensitivity compared to the [F_2/G/F_2] hybrid laminate implies that the position of glass fibres in the laminate have an effect on the overall performance. More impact resistance and higher flexural strength are some of the other outcomes when placing the glass fibres at the outer layer [31], [35].

For a flax dominant laminate, there is a minimum amount of glass fibre replacement before the effects become significant. Protecting the flax material with more durable glass fibres can be a better solution to the already existing applications of flax fibre as the improvements are without sacrificing the fatigue performance. However, the resulted hybrid laminate would be less nature friendly due to the use of synthetic fibres.

As Kretsis [46] states, hybrid composites should not be evaluated as being superior to single-fibre composites without considering the application. Instead, they can offer useful alternatives where single-fibre composites do not satisfy all the requirements of a structure. Hence, all aspects of a structural design should be considered while comparing different options. Aspects such as strength, stiffness, impact and fatigue resistivity, ease of manufacture and emissions during processing, carbon footprint, weight, cost and many more factors should be considered before making such comparison. It is only then that a hybrid can be selected as being superior to a single-fibre composite.

6. Conclusions

After performing an experimental investigation of the proposed hybrids in this research, several conclusions can be drawn in regards to the effect of hybridization in different cases. By partial replacement of flax fibres with glass fibres, the resulted flax dominant hybrid composite is capable of withstanding more loads with higher fatigue strength. It is important to realize that in the case of flax dominant hybrids a minimum amount of glass fibre is required before its effect appears in the hybrid laminate. This is especially apparent when specific (weight-normalized) properties are considered. Also, placing the glass fibres at the outer layers of the hybrid laminate seems to be advantageous when considering the reported improvements achieved by this type of stacking sequence in addition to the improvements seen in static and fatigue performance in this research. In the case of partial replacement of glass fibre with flax, while there is a reduction in the fatigue strength of the resulted laminate, it will become less fatigue sensitive which improves the fatigue life of the composite laminate at low load levels. Thus for low loading applications, adding flax fibre to the glass fibre in the laminate can create a more durable hybrid composite. Most importantly the effect of strain incompatibility should be taken into consideration, as it can cause severe internal damage, which highly affect the properties and functionality of the final product.

6.1. Major contributions

During the course of this study, some major contributions were made that were primarily results of the experimental nature of this study.

- A modified VARTM process was developed which is capable of creating high quality hybrid laminates in the presence of low permeability fibres such as flax fibres. This process can be further optimized to reduce the resin waste and potentially increase the fibre volume fraction.
- Contributing to the limited fatigue data available on natural fibres is another important achievement of this study. Furthermore, based on our knowledge, at the point of this writing there have been no similar studies on the fatigue performance of such hybrids using materials matching the quality of those used in this research. The aim was to use

real work imitated samples to create practical results that are close to the real world situations.

6.2. Future work

Due to the time limitations of this study there remain several aspects for further investigation and perhaps improving the results.

- Better manufacturing techniques can be utilized that allow more control over the fibre volume fraction to create parts with similar fibre fraction, such as RTM or the same infusion process used in this study followed by compression moulding, to have a better comparison between the behaviour of different compositions.
- Although fibre treatment has been reported to generate some improvements in the case of epoxy resin, chemical or surface treatment of fibres can be considered to enhance the interfacial properties of fibres and the resin system. This can result in a better load transfer between low-elongation and high-elongation fibres to create more ductile hybrid laminates.
- Further tests can be performed at lower levels of fatigue loading to potentially prove the hypothesis of better fatigue performance and lower damage accumulation in glass dominant hybrids at low load levels, as in $[G_2/F/G_2]$ hybrid laminate. Having information on the endurance limit of each composition can also be beneficial for designing parts requiring long lifetimes.

Appendices

Appendix I. Twist and crimp measurement

Twist and crimp are two important characteristics of a woven fabric. Crimp is an indication of the waviness of the fibres in a woven mat as the warp and weft fibre bundles intermingle with one another. Crimp index (Equation I-1) [50] is defined as an indicator of the crimp of a woven fabric for any type of fibre (synthetic or natural), and it is calculated based on the ratio of extendable length of a fibre over the extended length of that fibre. On the other hand, twist per meter (Equation I-2) [51] is only measurable for natural fibres due to their weaving process. Extracted continues fibres from plants such as flax are short in length, usually in the range of couple of centimeters. The short fibres are twisted to each other to form a lengthy yarn, which is then used in the weaving process.

$$C_i = \frac{L_o - P}{L_o} \qquad \text{Equation I-1}$$

L_o is the extended length of the fibre, which means the length of a straightened fibre. P is the length of a fibre as it is crimped and C_i is the crimp index. Figure I.1 is an example of polished samples used for crimp measurements. Six samples were used for crimp measurement.

Image analysis was used to measure the twist angle (θ), which is defined by the angle of the fibres from the yarn direction. Equation I-2 defines the twist per meter based on twist angle (θ) and yarn diameter (d). Ten measurements were made and the average is presented as the twist value of the fibres.

$$t = \frac{tan\ \theta}{\pi d} \qquad \text{Equation I-2}$$

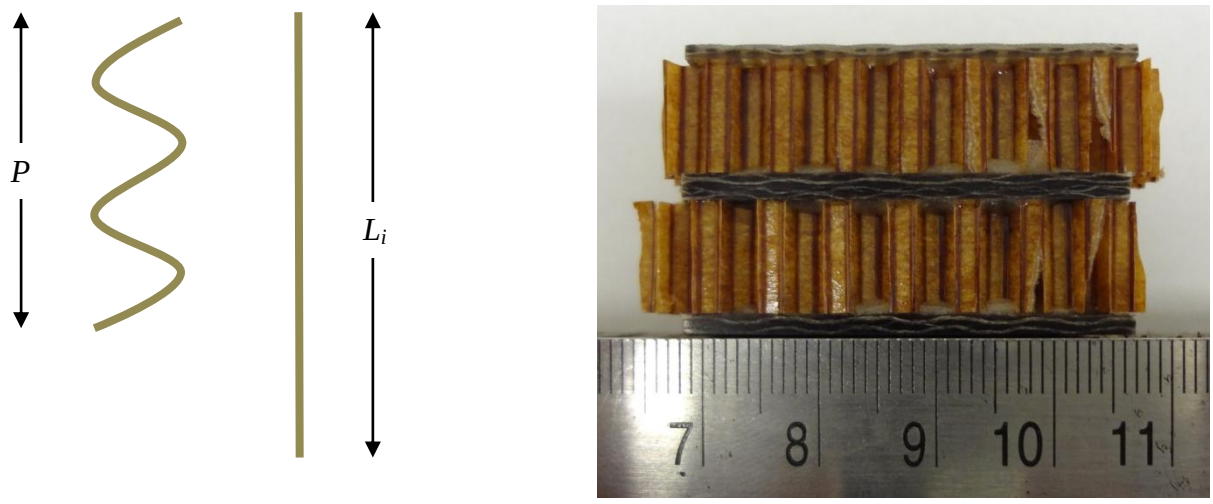

Figure I.1 Left picture: diagram for P and L_i. Right picture: cut and polished samples glued to honeycombs for taking microscopic images and measuring the crimp of flax fibres

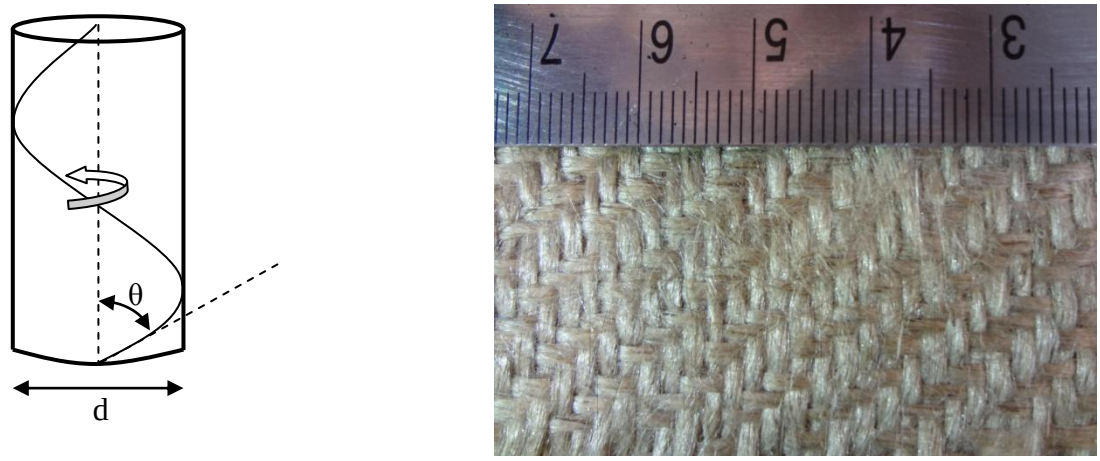

Figure I.2 Left picture: diagram showing a yarn and its parameters. Right picture: image taken by high resolution digital camera to measure the twist angle and yarn diameter

Appendix II. Indirect fibre volume fraction calculation

The volume fraction has been calculated based on the indirect method of calculation of the fibre content according to equations below:

$$W_f = W_{ff} + W_{fg} \quad \text{Equation II-3}$$

where W_{ff} is the fibre weight faction of flax fibres and W_{fg} is the fibre weight fraction of glass fibres.

W_{ff} is given by Equation II-4

$$W_{ff} = n\frac{W_f}{W_c} \quad \text{Equation II-4}$$

Where n is the number of flax fibre layers used in the laminate and W_f is the areal weight of the flax fabric, which was measured experimentally. W_c is the average weight per unit area of the composite.

Based on the same method W_{fg} is calculated by Equation II-5

$$W_{fg} = n\frac{W_g}{W_c} \quad \text{Equation II-5}$$

Again here n is the number of glass fibre mats used, and W_g is the areal weight of glass fibre mat, and W_c is the average weight per unit area of the composite.

Fibre volume fraction is then given by the following Equation II-6 and Equation II-7

$$V_f = \frac{\rho_c W_f}{\rho_f} \quad \text{Equation II-6}$$

$$V_g = \frac{\rho_c W_g}{\rho_g} \quad \text{Equation II-7}$$

Here V_f and V_g represent the volume fraction of flax fibre and glass fibre, respectively. ρ_c is the density of the corresponding laminate, and ρ_f and ρ_g are densities of the flax fibre and the glass fibre, which assumed to be 1.498 g/cm^3 [43] and 2.6 g/cm^3 [15] respectively.

Appendix III. Microscopic image analysis for assessing void content

Microscopic image analysis was used to measure the void content. 4 cm samples were cut from randomly selected coupons. Due to limited resources, only one coupon was selected from each composition to present its population. Multiple images were taken from the cross-section of well-polished samples at the magnification of X50 using the digital camera mounted on the microscope (Figure III.3). Afterwards, pictures were stitched together using Adobe Photoshop software to create a panoramic view of the samples (Figure III.4). Freeware ImageJ software was used to analyze the stitched images by converting them to 8-bit grayscale. A threshold function was applied to isolate the manually selected void regions, whose area was measured by the software. While this is not a standard way of assessing amount of voids in a laminate, due to high sources of human error, it is generally accepted that it can provide adequate information on judging a part's quality and locating sizable defects.

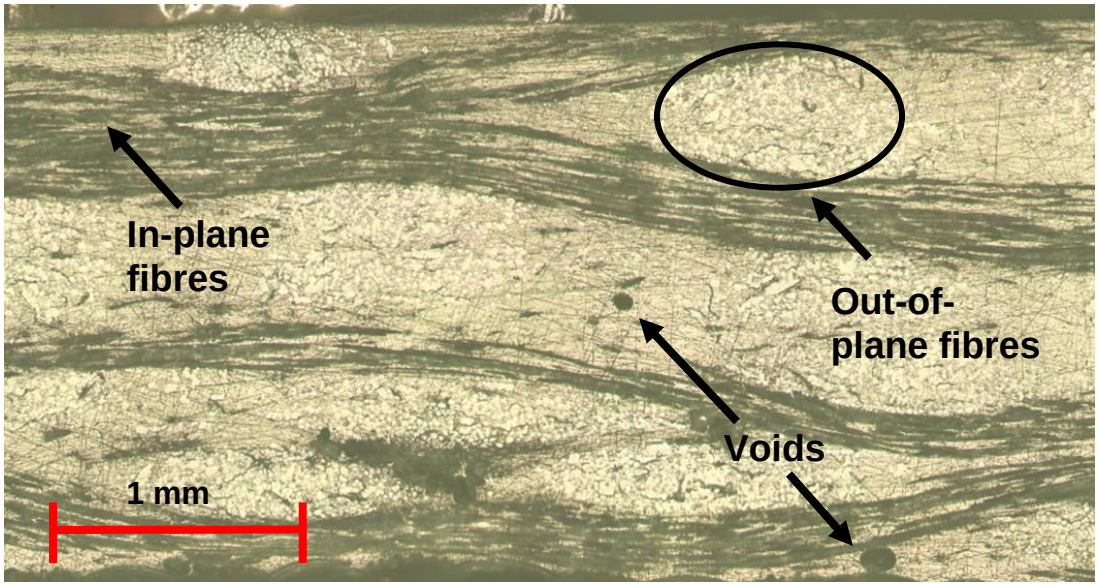

Figure III.3 Microscopic image of the cross section of a [F_5] sample

(a)

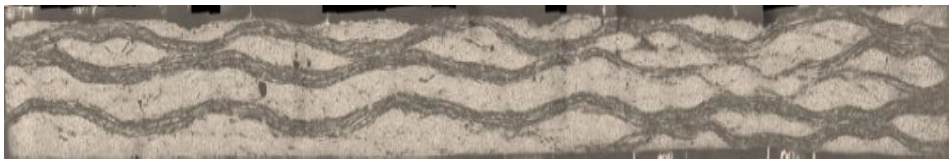

(b)

(c)

(d)

(e)

Figure III.4 Stiched microscopic images for different compositions. (a) [F_5], (b) [$F_2/G/F_2$], (c) [$G/F_3/G$], (d) [$G_2/F/G_2$] and (e) [G_5]

Appendix IV. S-N curve plotting based on logarithmic linear curve fit

The general equation used to construct the S-N curve in this report is based on the assumption that the logarithm of the fatigue life is normally distributed, and that the variance of the log life is constant in the entire range of the testing. This linear relationship can be defined as equation below.

$$\log N = A + B(S) \qquad \text{Equation IV-8}$$

Here, log N is considered to be a dependent variable and can be replaced by 'Y'. A and B are maximum likelihood estimators. Since B is a function of independent variable S or the stress, the equation can be rewritten as:

$$Y = A + BX \qquad \text{Equation IV-9}$$

As mentioned above, Y is the dependent variable and X represents the independent variable, which is the stress value. A and B are fitting parameters where the estimated version of these variables can be defined as below.

$$\hat{A} = \bar{Y} - \hat{B}\bar{X} \qquad \text{Equation IV-10}$$

$$\hat{B} = \frac{\sum_{i=1}^{k}(X_i - \bar{X})(Y_i - \bar{Y})}{\sum_{i=1}^{k}(X_i - \bar{X})^2} \qquad \text{Equation IV-11}$$

Where the $\bar{Y}$ and $\bar{X}$ indicate the average value of stress and log N, and k is the number of samples tested.

Based on the same parameters, the variance can be defined as in Equation IV-12

$$\hat{\sigma}^2 = \frac{\sum_{i=1}^{k}\left(Y_i - \hat{Y}_i\right)^2}{k-2} \qquad \text{Equation IV-12}$$

Where the $\hat{Y}_i = \hat{A} + \hat{B}X_i$ and Y_i is the independent variable calculated from Log N. When k is the number of samples tested, the $k-2$ in the denominator makes $\hat{\sigma}^2$ an unbiased estimator of the normal population variance σ^2.

Appendix V. Confidence band for the entire median S-N curve

The confidence bands are based on the t-distribution, which gives the estimator values a confidence level. The equation for the confidence band for the entire median is described below, where *Y'* corresponds to the dependence values of confidence bands.

$$Y' = \hat{A} + \hat{B}X \pm \sqrt{2F_p}\hat{\sigma}\left[\frac{1}{k} + \frac{(X-\bar{X})^2}{\sum_{i=1}^{k}(X_i-\bar{X})^2}\right]^{\frac{1}{2}} \qquad \text{Equation V-13}$$

In the equation above, the $\hat{A} + \hat{B}X$ section of the equation present the linear curve fitting values, which can be used from the previous section. F_p is a statistical parameter defined by statistical degree of freedom. The values for this constant can be found on Table 2 of the ASTM E739-10 standard. $\hat{\sigma}$ is the estimated standard deviation and k is the number of tested samples.

The degrees-of-freedom for all cases in this research were n_1=2, and n_2=10 which is defined by k-2. Consequently, the value for F_p taken form Table 2 is 4.1028.

Appendix VI. Testing the adequacy of the linear model

The linearity of data points for each tested laminate was calculated based on the equation below, under the condition that the value calculated from this equation does not exceed the F_P value from Table 2 of ASTM E739-10. Statistical degrees-of-freedom for this table are n_1 and n_2 defined as n_1=l-2 and n_2=k-l, where l indicates the number of different levels that the samples were tested and k is the total number of samples.

$$F = \frac{\sum_{i=1}^{l} m_i(\hat{Y}_i - \bar{Y}_i)^2/(l-2)}{\sum_{i=1}^{l}\sum_{j=1}^{m_i}\left(Y_{ij} - \bar{Y}_i\right)^2/(k-l)} \qquad \text{Equation VI-14}$$

In the equation above m_i is the number of replications of $\hat{Y}$ at each X_i. Other terms are defined as before. Values calculated from this equation for each laminate are listed in the table below.

Table VI.1 List of calculated values from Equation VI-14

Layup	**Calculated values of F**
$[F_5]$	2.432
$[F_2/G/F_2]$	5.066
$[G/F_3/G]$	0.8177
$[G_2/F/G_2]$	1.895
$[G_5]$	1.574

Since data for all laminates has the same degrees of freedom, the F_P value from Table 2 of mentioned standard will be the same. All calculated values listed in table above are less than F_P=5.1174, thus linear assumption is valid for all data sets.

Appendix VII. The specific stress-number of cycles to failure (S-N) curves

Graphs below show the S-N curves for all laminates. In all graphs, dots represent the actual data extracted from tests in term of final number of cycle to failure and the maximum stress applied to the sample, blue linear lines are the linear curve fits and dashed lines are the 95% confidence bands. While the axes are same in all graphs, the range varies between them. The y-axes are stress in MPa and x-axes are the number of cycles on a logarithmic scale.

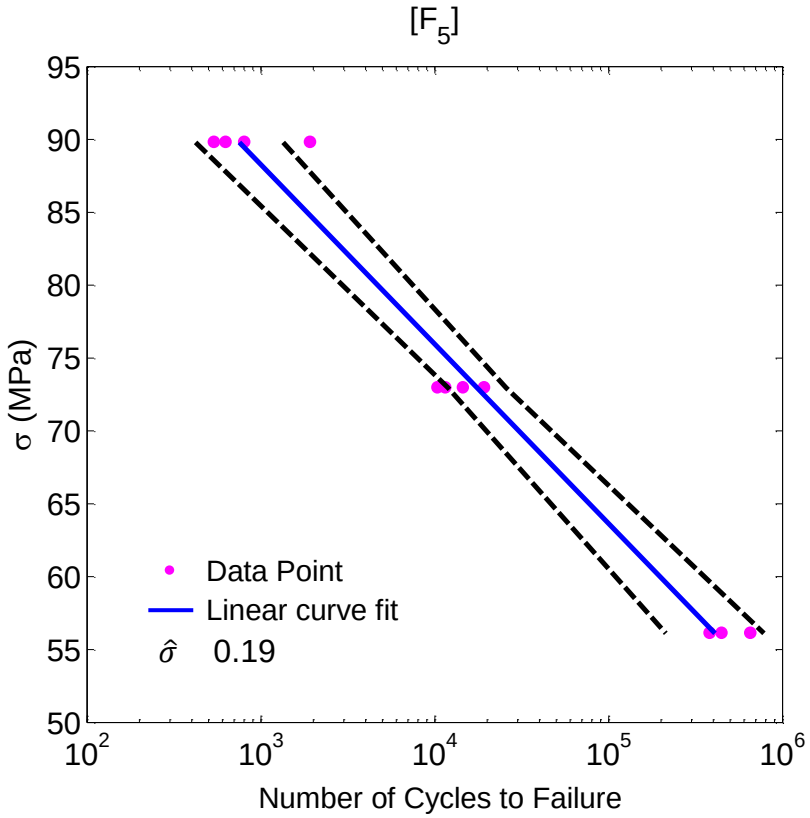

Figure VII.5 S-N curve for FFRE non-hybrid laminate

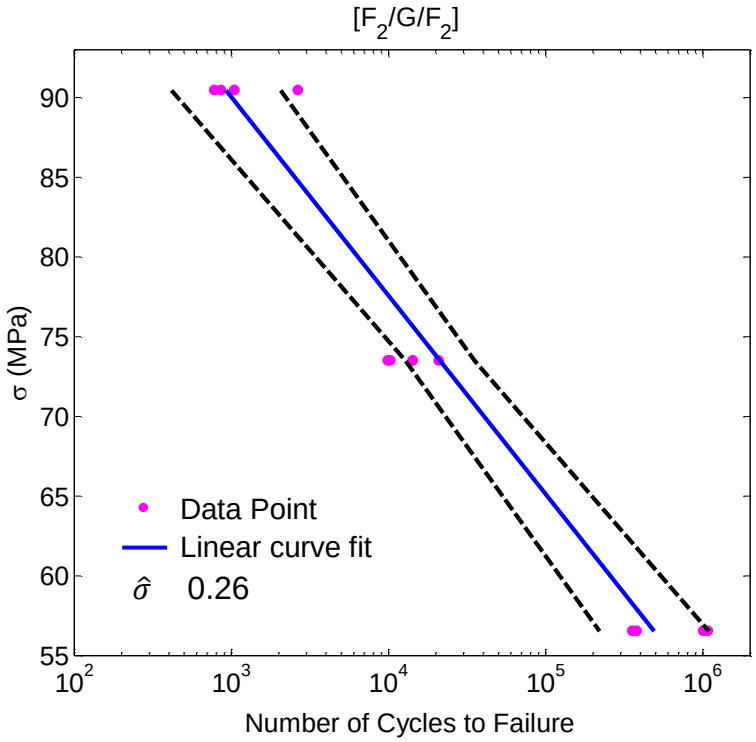

Figure VII.6 S-N curve for $[F_2/G/F_2]$ hybrid laminate

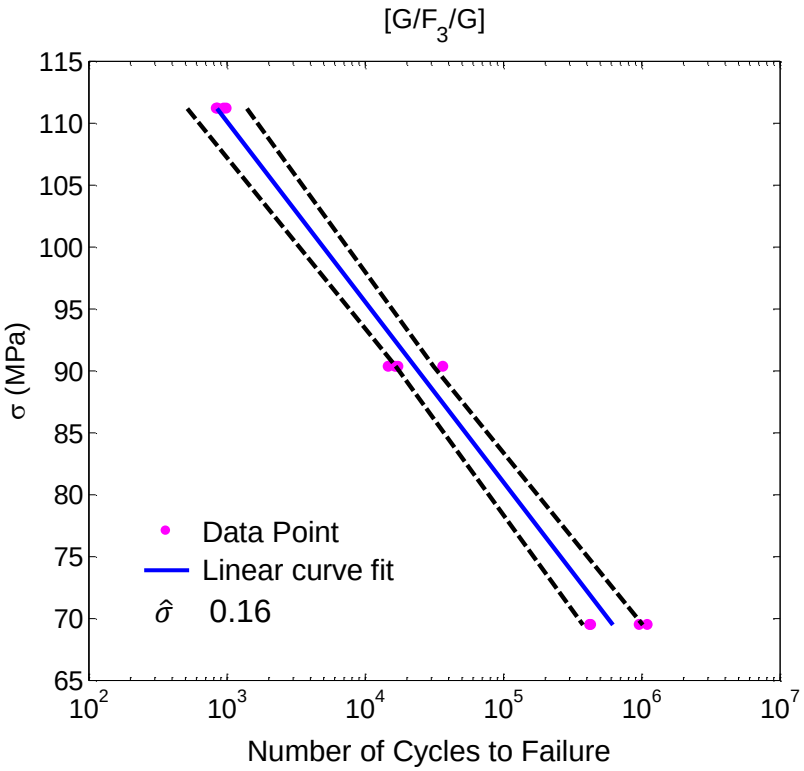

Figure VII.7 S-N curve for $[G/F_3/G]$ hybrid laminate

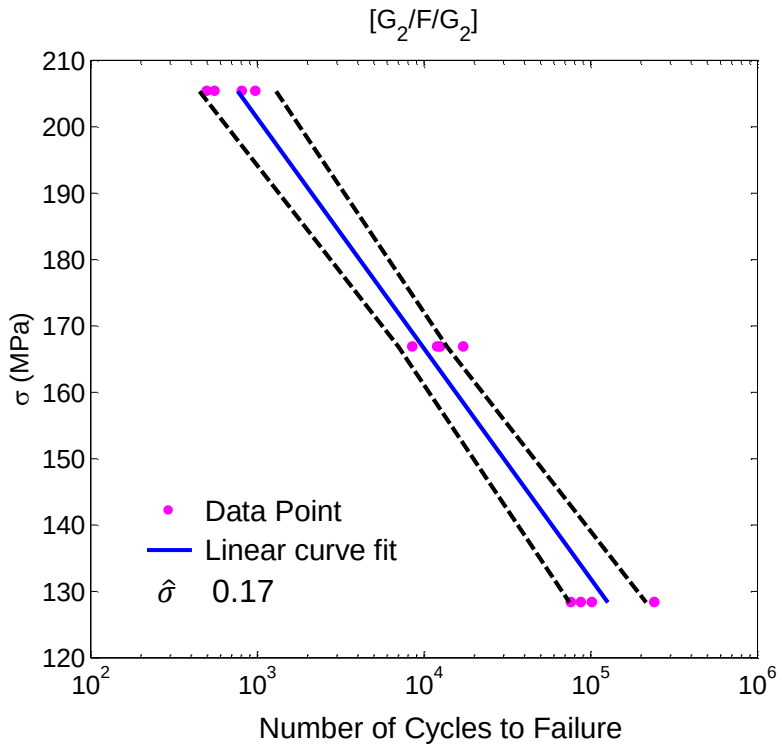

Figure VII.8 S-N curve for $[G_2/F/G_2]$ hybrid laminate

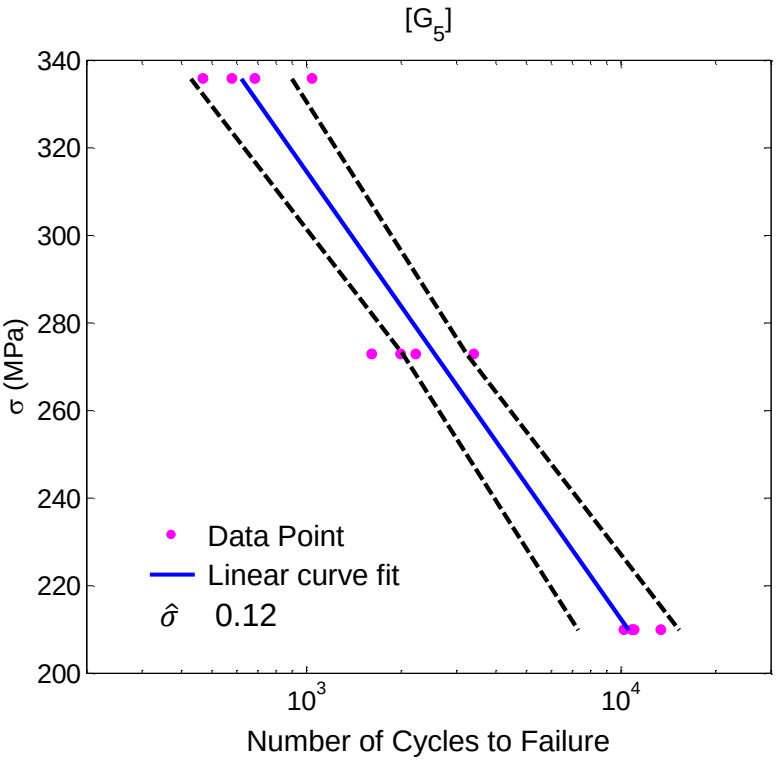

Figure VII.9 S-N curve for GFRE non-hybrid laminate

Appendix VIII Resin data sheet.

820 Marine epoxy laminating system info sheet.

Test	**Test Method**	**820/824**
Mix Ratio	By Weight	100R:18H
Mix Ratio	By Volume	5R:1H
Mixed Viscosity	Brookfield	425 cps
Pot Life	Minutes	50-60
Mixed Density	lbs/gal	9.13
Mixed Density	lbs/in_3	0.04
Specific Gravity	gm/cc	1.09
Demold Time	Hours	24
V.O.C.	g/L	0.0
Minimum Cure Schedule	Hours	24
Complete Cure Schedule	Days	7
Tensile Strength	ASTM D-638.946	45,000 psi
*Tensile Elongation	ASTM D-638.946	2.0%
Tensile Modulus	ASTM D-638.946	3,000,000 psi
Flexural Strength	ASTM D-790.92	45,000 psi
Flexural Modulus	ASTM D-790.92	2,200,000 psi
*Compressive Strength	ASTM D-695.91	8,400 psi
*Compressive Modulus	ASTM D-695.91	160,000 psi
*Impact Strength	ASTM D-256.93a	3.75 (in-lbf/in)
*HDT @ 66 PSI	ASTM D-648.82	72°C/161°F
*Average Moisture Absorption	ASTM D-570.81	0.25%

References

[1] R. D. Anandjiwala and S. Blouw, "Composites from bast fibres-Prospects and potential in the changing market environment," *Journal of Natural Fibers,* vol. 4, pp. 91-109, 2007.

[2] T. Corbiere-Nicollier, B. Gfeller-Laban, L. Lundquist, Y. Leterrier, J. A. E. Manson, and O. Jolliet, "Life cycle assessment of biofibres replacing glass fibres as reinforcement in plastics," *Resources Conservation and Recycling,* vol. 33, pp. 267-287, Nov 2001.

[3] D. N. Saheb and J. P. Jog, "Natural fiber polymer composites: A review," *Advances in Polymer Technology,* vol. 18, pp. 351-363, 1999.

[4] D. B. Dittenber and H. V. GangaRao, "Critical review of recent publications on use of natural composites in infrastructure," *Composites Part A: Applied Science and Manufacturing,* vol. 43, pp. 1419-1429, 2012.

[5] E. P. Rodriguez, R. Puglia, D. , "Characterization of Composites Based on Natural and Glass Fibers Obtained by Vacuum Infusion," *Journal of Composite Materials,* vol. 39, pp. 265-282, 2005.

[6] (May 14, 2013). Available: www.flaxcouncil.ca

[7] J. K. Pandey, S. Ahn, C. S. Lee, A. K. Mohanty, and M. Misra, "Recent advances in the application of natural fiber based composites," *Macromolecular Materials and Engineering,* vol. 295, pp. 975-989, 2010.

[8] M.-p. Ho, H. Wang, J.-H. Lee, C.-k. Ho, K.-t. Lau, J. Leng, *et al.,* "Critical factors on manufacturing processes of natural fibre composites," *Composites Part B: Engineering,* vol. 43, pp. 3549-3562, 12// 2012.

[9] N. Reddy and Y. Yang, "Biofibers from agricultural byproducts for industrial applications," *TRENDS in Biotechnology,* vol. 23, pp. 22-27, Jan 2005.

[10] R. Malkapuram, V. Kumar, and Y. S. Negi, "Recent development in natural fiber reinforced polypropylene composites," *Journal of Reinforced Plastics and Composites,* vol. 28, pp. 1169-1189, 2009.

[11] L. B. Yan, N. Chouw, and K. Jayaraman, "Flax fibre and its composites - A review," *Composites Part B-Engineering,* vol. 56, pp. 296-317, Jan 2014.

[12] S. Alix, E. Philippe, A. Bessadok, L. Lebrun, C. Morvan, and S. Marais, "Effect of chemical treatments on water sorption and mechanical properties of flax fibres," *Bioresource Technology,* vol. 100, pp. 4742-4749, 10// 2009.

[13] J. Morales, M. Olayo, G. Cruz, P. Herrera-Franco, and R. Olayo, "Plasma modification of cellulose fibers for composite materials," *Journal of applied polymer science,* vol. 101, pp. 3821-3828, 2006.

[14] D. Rouison, "Resin transfer molding of natural fiber reinforced plastics," NR06881 Ph.D., University of New Brunswick (Canada), Ann Arbor, 2004.

[15] S. V. Joshi, L. T. Drzal, A. K. Mohanty, and S. Arora, "Are natural fiber composites environmentally superior to glass fiber reinforced composites?," *Composites Part A: Applied Science and Manufacturing,* vol. 35, pp. 371-376, 2004.

[16] S. Nunna, P. R. Chandra, S. Shrivastava, and A. Jalan, "A review on mechanical behavior of natural fiber based hybrid composites," *Journal of Reinforced Plastics and Composites,* vol. 31, pp. 759-769, 2012.

[17] E. S. Greenhalgh, *Failure analysis and fractography of polymer composiets*. Cambridge: Woodhead publishing limited, 2009.

[18] M. Jawaid and H. P. S. Abdul Khalil, "Cellulosic/synthetic fibre reinforced polymer hybrid composites: A review," *Carbohydrate Polymers,* vol. 86, pp. 1-18, 2011.

[19] T.-W. Chou and J. L. Nowinski, "Microstructural design of fiber composites," in *Proceedings of the 1996 Symposium on Micromechanics of Advanced Materials, October 29, 1995 - November 2, 1995*, Cleveland, OH, USA, 1995, pp. 413-419.

[20] H. Fukuda and T. W. Chou, "Monte-Carlo Simulation of the Strength of Hybrid Composites," *Journal of Composite Materials,* vol. 16, pp. 371-385, 1982.

[21] G. Marom, S. Fischer, F. R. Tuler, and H. D. Wagner, "Hybrid Effects in Composites - Conditions for Positive or Negative Effects Versus Rule-of-Mixtures Behavior," *Journal of Materials Science,* vol. 13, pp. 1419-1426, 1978.

[22] M. M. Thwe and K. Liao, "Effects of environmental aging on the mechanical properties of bamboo-glass fiber reinforced polymer matrix hybrid composites," *Composites Part a-Applied Science and Manufacturing,* vol. 33, pp. 43-52, 2002.

[23] M. S. Sreekala, J. George, M. G. Kumaran, and S. Thomas, "The mechanical performance of hybrid phenol-formaldehyde-based composites reinforced with glass and oil palm fibres," *Composites Science and Technology,* vol. 62, pp. 339-353, 2002.

[24] A. Atiqah, M. A. Maleque, M. Jawaid, and M. Iqbal, "Development of kenaf-glass reinforced unsaturated polyester hybrid composite for structural applications," *Composites Part B: Engineering,* vol. 56, pp. 68-73, 1// 2014.

[25] H. P. S. Aabdul Khalil, C. W. Kang, A. Khairul, R. Ridzuan, and T. Adawi, "The effect of different laminations on mechanical and physical properties of hybrid composites," *Journal of Reinforced Plastics and Composites,* vol. 28, pp. 1123-1137, 2009.

[26] K. Sabeel Ahmed and S. Vijayarangan, "Tensile, flexural and interlaminar shear properties of woven jute and jute-glass fabric reinforced polyester composites," *Journal of Materials Processing Technology,* vol. 207, pp. 330-335, Oct 16 2008.

[27] G. Cicala, G. Cristaldi, G. Recca, G. Ziegmann, A. El-Sabbagh, and M. Dickert, "Properties and performances of various hybrid glass/natural fibre composites for curved pipes," *Materials and Design,* vol. 30, pp. 2538-2542, 2009.

[28] B. Harris, *Fatigue in Composites-Science and technology of the fatigue response of fibre-reinforced plastics*. Boca Raton: CRC Press, 2003.

[29] M. M. Thwe and K. Liao, "Durability of bamboo-glass fiber reinforced polymer matrix hybrid composites," *Composites Science and Technology,* vol. 63, pp. 375-387, 2003.

[30] P. Reis, J. Ferreira, F. Antunes, and J. Costa, "Flexural behaviour of hybrid laminated composites," *Composites Part A: Applied Science and Manufacturing,* vol. 38, pp. 1612-1620, 2007.

[31] A. Shahzad, "Impact and fatigue properties of hemp-glass fiber hybrid biocomposites," *Journal of Reinforced Plastics and Composites,* vol. 30, pp. 1389-1398, 2011.

[32] T. Yuanjian and D. H. Isaac, "Impact and fatigue behaviour of hemp fibre composites," *Composites Science and Technology,* vol. 67, pp. 3300-3307, 12// 2007.

[33] S. Liang, P. B. Gning, and L. Guillaumat, "A comparative study of fatigue behaviour of flax/epoxy and glass/epoxy composites," *Composites Science and Technology,* vol. 72, pp. 535-543, 2012.

[34] A. A. Fotouh, J. D. Wolodko, and M. G. Lipsett, "Fatigue Behavior of Natural Fiber Reinforced Thermoplastic " *Composites: Part B,* pp. 71-77, 19 Feb, 2014 2014.

[35] C. Santulli, M. Janssen, and G. Jeronimidis, "Partial replacement of E-glass fibers with flax fibers in composites and effect on falling weight impact performance," *Journal of Materials Science,* vol. 40, pp. 3581-3585, Jul 2005.

[36] Q. Govignon, S. Bickerton, and P. A. Kelly, "Simulation of the reinforcement compaction and resin flow during the complete resin infusion process," *Composites Part A: Applied Science and Manufacturing,* vol. 41, pp. 45-57, 2010.

[37] D. Heider and J. W. Gillespie, "VARTM Variability and Substantiation," ed, 2008.

[38] C. Niggemann, S. S. Young, J. W. Gillespie, and D. Heider, "Experimental investigation of the controlled atmospheric pressure resin infusion (CAPRI) process," *Journal of Composite Materials,* vol. 42, pp. 1049-1061, Jun 2008.

[39] S. Phillips, J. Baets, L. Lessard, P. Hubert, and I. Verpoest, "Characterization of flax/epoxy prepregs before and after cure," *Journal of Reinforced Plastics and Composites,* vol. 32, pp. 777-785, 2013.

[40] A. N. Towo and M. P. Ansell, "Fatigue evaluation and dynamic mechanical thermal analysis of sisal fibre–thermosetting resin composites," *Composites Science and Technology,* vol. 68, pp. 925-932, 2008.

[41] A. Hammami, "Key factors affecting permeability measurement in the vacuum infusion molding process," *Polymer Composites,* vol. 23, pp. 1057-1067, Dec 2002.

[42] F. Robitaille and R. Gauvin, "Compaction of textile reinforcements for composites manufacturing. I: Review of experimental results," *Polymer Composites,* vol. 19, pp. 198-216, Apr 1998.

[43] P. B. Gning, S. Liang, L. Guillaumat, and W. J. Pui, "Influence of process and test parameters on the mechanical properties of flax/epoxy composites using response surface methodology," *Journal of Materials Science,* vol. 46, pp. 6801-6811, 2011.

[44] "Standard Test Method for Tension-Tension Fatigue of Polymer Matrix Composite Materials," in *Annual Book of ASTM Standards*, ed, 2012.

[45] "Standard Test Method for Tensile Properties of Polymer Matrix Composite Materials," in *Annual book of ASTM Standards*. vol. 15.03, ed, 2012, pp. 81-93.

[46] G. Kretsis, "A Review of the Tensile, Compressive, Flexural and Shear Properties of Hybrid Fiber-Reinforced Plastics," *Composites,* vol. 18, pp. 13-23, Jan 1987.

[47] "Standard Practice for Statistical Analysis of Linear orLinearized Stress-Like (S-N) and Strain-Life (eps-N) Fatigue Data " in *Annual Book of ASTM Standards*. vol. 03.01, ed, 2012, pp. 721-727.

[48] A. Greco, C. Musardo, and A. Maffezzoli, "Flexural creep behaviour of PP matrix woven composite," *Composites Science and Technology,* vol. 67, pp. 1148-1158, 5// 2007.

[49] C. Baley, "Analysis of the flax fibres tensile behaviour and analysis of the tensile stiffness increase," *Composites Part a-Applied Science and Manufacturing,* vol. 33, pp. 939-948, 2002.

[50] R. H. Brand and S. Backer, "Mechanical Principles of Natural Crimp of Fiber," *Textile Research Journal,* vol. 32, pp. 39-49, 1962.

[51] J. Bogdan, "The characterization of spinning quality," *Textile Research Journal,* vol. 26, pp. 720-730, 1956.